RICE UNIVERSITY

AN ANALYTICAL STUDY OF THE BEHAVIOR OF PRESTRESSED COMPOSITE BEAMS

by

Ronald Steven Reagan

A THESIS SUBMITTED
IN PARTIAL FULFILLMENT OF THE
REQUIREMENTS FOR THE DEGREE OF

MASTER OF SCIENCE

Thesis Director's signature:

Nat W. Krahl

Houston, Texas
May, 1966

RONALD STEVEN REAGAN

ABSTRACT

This thesis presents an analytical study of the behavior of prestressed composite beams. The particular configuration of prestressed composite beam considered is a simply-supported steel beam, prestressed by a high-strength steel tendon with a constant eccentricity, and attached to a concrete slab by shear connectors designed to insure complete interaction.

A numerical method for analyzing the statically indeterminate beam was developed and used as a basis for a computer program which found the strains and deflections at a discrete number of equally spaced points along the length of the beam for increasing values of load up to the failure load. These strains and deflections satisfied the stress-strain relations for the materials, the static equilibrium of the beam, and the compatibility of deformation of the tendon. Hognestad's stress-strain relation was assumed for the concrete slab, an elasto-plastic stress-strain relation was assumed for the steel beam, and an actual stress-strain curve was used for the tendon. The numerical procedure combines the method of tangents for solving simultaneous nonlinear equations with a method of successive approximations. A simplification of this program was devised to analyze conventional composite beams.

Detailed studies were made of some prestressed composite beams suitable for highway bridges and some suitable for buildings. The effect on behavior of variation of prestress force and tendon size were investigated and compared with the effect of variation of cover plate size for conventional composite beams. These studies show that prestressing a composite beam is an effective means of increasing the load capacity of the beam at all of the following stages of behavior: load causing allowable steel stress, load causing yielding of steel beam, and ultimate load. Prestressing does

not significantly increase the load causing the allowable concrete stress nor does it significantly reduce live load deflection. The behavior of a prestressed composite beam is shown to be not very sensitive to variation of slab thickness.

The validity of the method of analysis was verified by the comparison of analytical and experimental results for several prestressed and conventional composite beams which were tested in the laboratory by other investigators.

TABLE OF CONTENTS

ACKNOWLEDGMENT

The author sincerely appreciates the encouragement, guidance, and assistance given by Dr. Nat W. Krahl, Associate Professor of Structural Engineering.

LIST OF FIGURES

LIST OF FIGURES (cont'd)

LIST OF TABLES

1. INTRODUCTION

The structural element considered in this study is a simply-supported steel beam, unshored and prestressed by high-strength steel tendons with a constant eccentricity along the length of the steel beam, and with a concrete slab attached to the steel beam by shear connectors as shown in Fig. 1. This structural element is assumed for design purposes to approximate the behavior of prestressed steel beam and one-way slab systems for bridges and buildings, when shear connectors are provided to insure composite action.

Prestressed composite beams have been studied by several authors. In 1949, F. Dischinger(1) published a series of articles proposing the prestressing of entire bridges by means of high-strength cables. In 1950, L. Coff(2) was granted a U. S. patent for a composite steel beam and concrete slab system prestressed by means of draped cables. The analysis of prestressed composite beams using both elastic assumptions and approximate ultimate strength methods was discussed in papers by R. Szilard(3) and P. G. Hoadley(4). Hoadley's method of ultimate strength analysis was approximate in that the statically indeterminate tendon force corresponding to the ultimate load of the composite section was not determined from consideration of equilibrium and compatibility of deformation, but was assumed to equal the tendon force at first yield of the steel beam. Comparisons were made by Hoadley between the moment capacities of conventional and prestressed composite beams.

Prestressed composite beams have been used in both bridge and building construction. A highway bridge near Des Moines, Iowa, was prestressed by jacking rolled steel beams into deflected shapes and welding high-strength

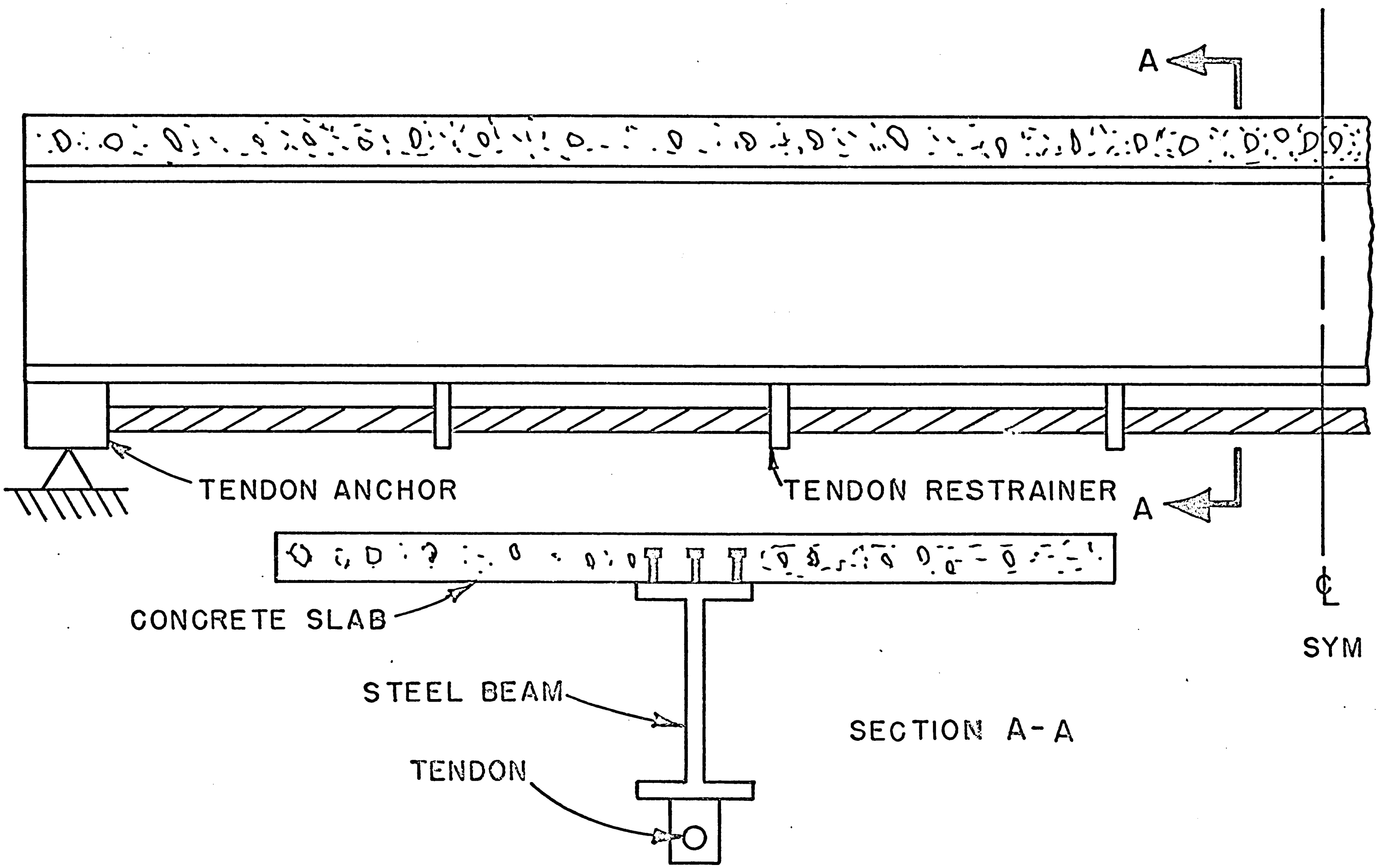

FIG. 1. Schematic diagram of a prestressed composite beam

cover plates onto their bottom flanges[5]. The roof system over a parking garage in Berkeley, California, was constructed using steel girders prestressed by the Prescon system and designed for composite action with a post-tensioned concrete slab[6]. A highway bridge near Brits in Transvaal, South Africa, was built using the Freyssinet system to prestress steel box girders which were connected by shear connectors to a cast-in-place concrete slab[7].

No published results of tests on prestressed composite beams could be found by the author, but test results for three identical prestressed composite beams did appear in a thesis by J. C. Stras, III[8].

The objectives of this study were as follows:

1. To determine from an analysis based on equilibrium and compatibility of deformation the behavior of prestressed composite beams throughout the entire range of loading up failure.
2. To compare the behavior of prestressed composite beams to the behavior of conventional composite beams with cover plates.
3. To determine the effect of variation of the prestress force and the slab thickness on the behavior of prestressed composite beams.
4. To analyze conventional and prestressed composite beams for which test results are available and then compare the analytical and experimental results.

2. METHOD OF ANALYSIS

A simply-supported prestressed composite beam is statically indeterminate internally to the first degree and is composed of three materials, structural steel, concrete, and high-strength steel, each with nonlinear relations between stress and strain. The method used to analyze this structure is a numerical procedure for solving simultaneously the equations of static equilibrium of the beam and compatibility of deformation of the prestressing tendon. A Fortran program based on the procedure was written for an IBM 7040 computer to carry out the computations presented in this thesis. The approach is somewhat similar to the method used by E. O. Pfrang and C. P. Siess[9] to analyze restrained reinforced concrete columns, in that it yields the same information, i. e., strains and deflections for values of applied load up to the failure load, that would be obtained from an actual structural test.

Assumptions

The assumptions used in the analysis were as follows:

1. Stress-strain relations

   a. Steel beam. For the steel beam the familiar elasto-plastic relationship as shown in Fig. 2(a) was assumed.

   b. Concrete slab. Hognestad's[10] stress-strain relationship as shown in Fig. 2(b) was assumed for the concrete slab. The concrete was assumed to take no tensile stress. The strain ϵ_o corresponding to the maximum concrete stress f''_c, which was assumed equal to 0.85 times the cylinder strength f'_c, was found from Eqs. 1 and 2.

$$E_c = 1.8x10^6 + 460f'_c \qquad (1)$$

$$\epsilon_o = 2f'_c/E_c \qquad (2)$$

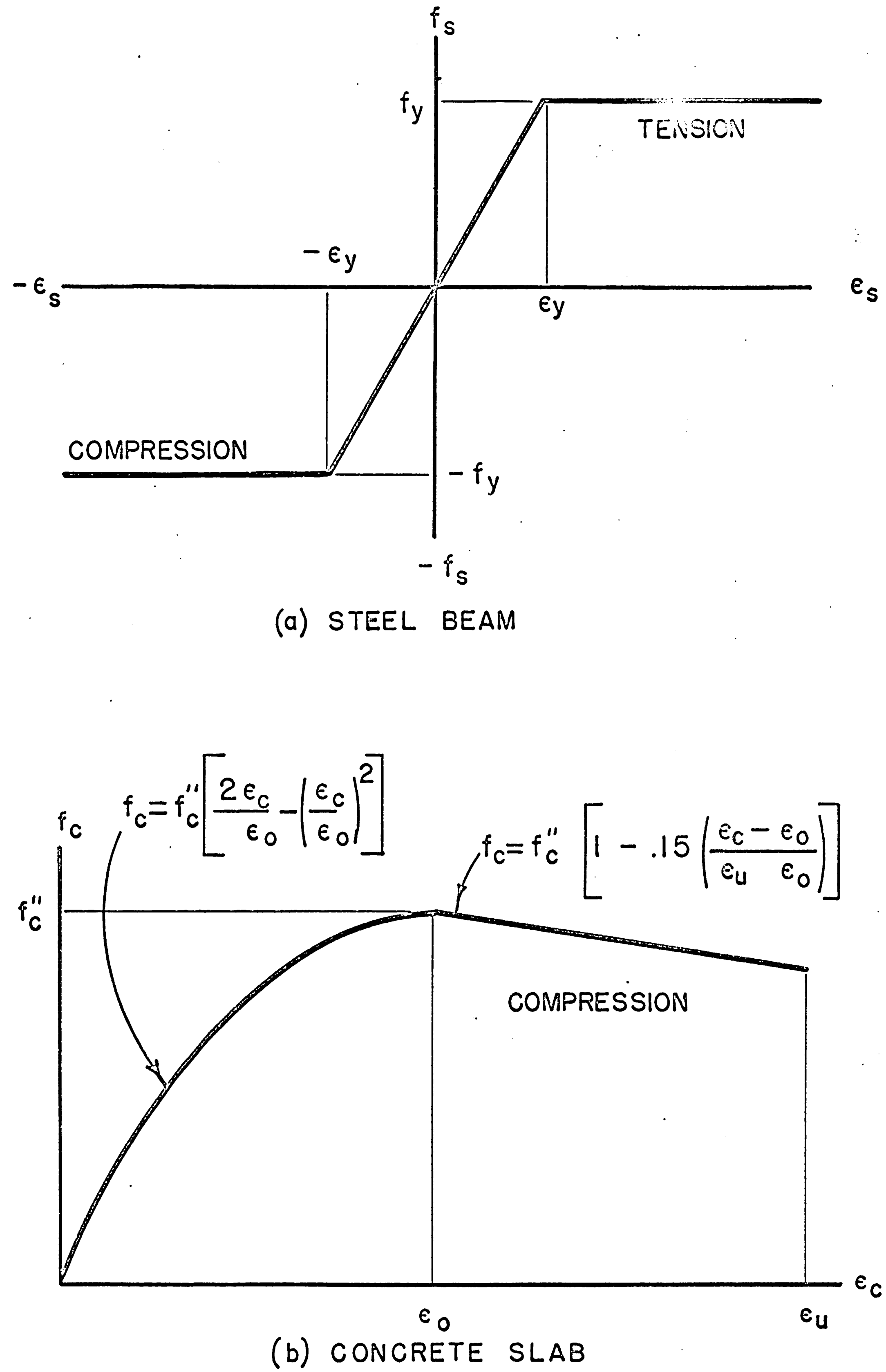

FIG. 2. Stress-strain relationships for steel beam and concrete slab

where E_c = initial tangent modulus of elasticity of concrete

c. Prestressing tendon. A table of discrete points from an actual stress-strain curve such as the one shown in Fig. 3 was assumed for the tendon. Parabolic interpolation was used at points intermediate to the table values.

2. Deformations caused by shear, creep, shrinkage, and tendon relaxation were neglected.
3. The cross section of the steel beam was treated as a number of rectangles.
4. Residual stresses in the steel beam were neglected.
5. The strain distribution across the cross section of the concrete slab and steel beam was assumed to be linear.
6. Complete interaction was assumed between the concrete slab and steel beam, i. e., no slip.
7. The prestressing tendon was restrained axially only at its ends and vertically to remain a constant distance from the steel beam.
8. Small angle theory was assumed.

General description of the method of analysis

The method of analysis used was incremental; that is, strains, deflections, and tendon force were found for increasing values of applied load, from no load to the failure load of the beam, which was assumed to occur when the concrete strain reached the ultimate concrete strain ϵ_u or the tendon reached its ultimate load. Initially a load increment approach was tried in which the applied load was incremented until failure, but this procedure was unsuccessful when a decrease in load occurred with increasing deflection. This is analogous physically to the difficulty in measuring the "downhill" side of the behavior of structures tested by

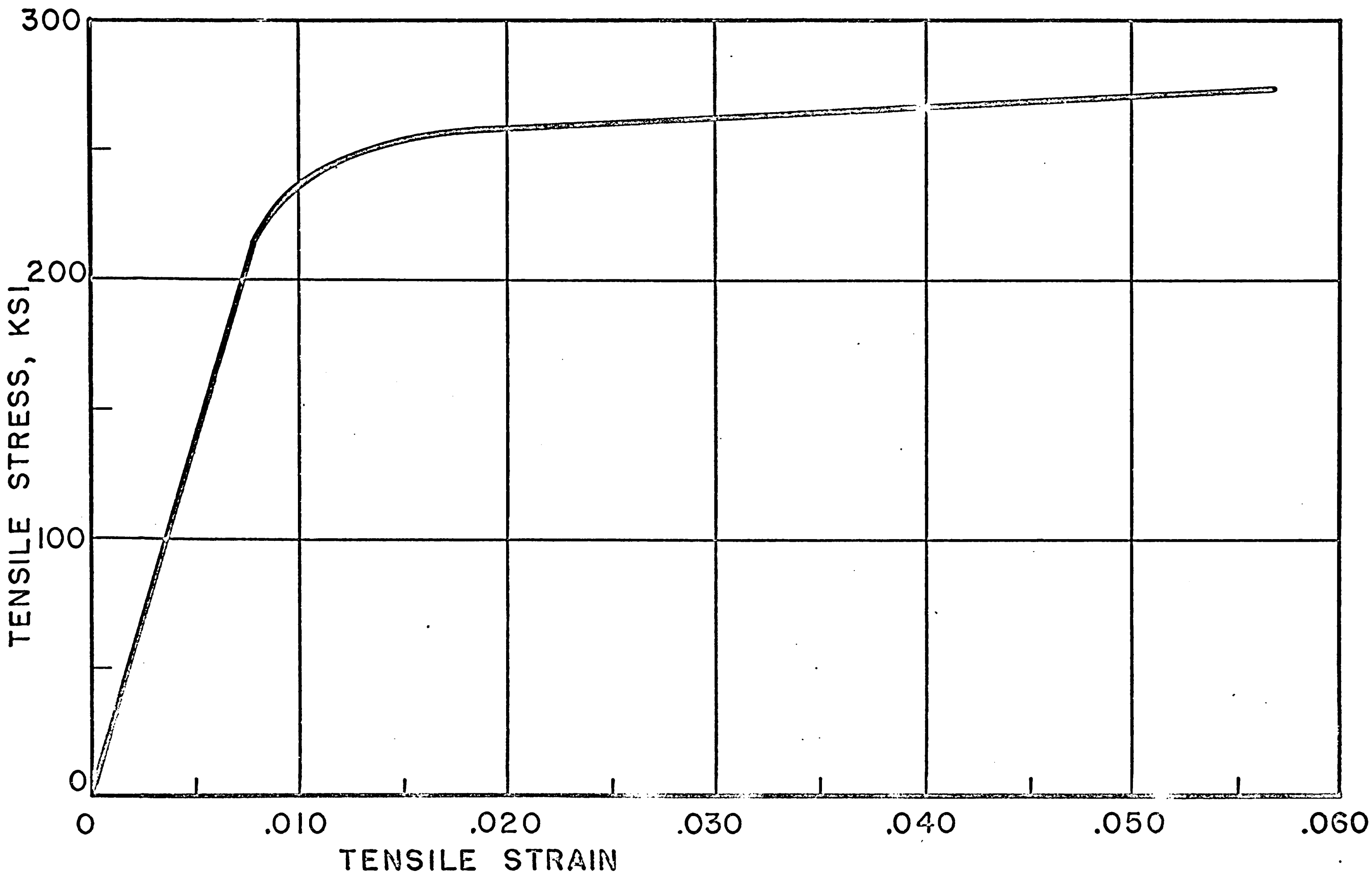

FIG. 3. Stress-strain relationship for a high-strength steel tendon

applying increments of load, as opposed to applying increments of deformation. This difficulty was overcome by incrementing a deformation, the strain at the bottom fiber of the steel beam at midspan, until failure of the beam.

Throughout the rest of this thesis the term "initial" will be used to refer to the effects of prestressing and dead load, i. e., before the application of live load. The dead load of the structure produces a parabolic distribution of moments to be carried by the steel beam, the concrete slab being initially unstressed as unshored construction was assumed. This causes each cross section of the prestressed composite beam to have a different initial strain distribution. Since the response of a cross section of a beam with a nonlinear stress-strain relationship depends on the initial strains, each cross section has a different relationship between applied forces and moments and deformations. Therefore instead of using stored tables of moment, axial load, curvature, and axial strain for every cross section of the beam, the equations of static equilibrium were solved to find the deformation of the beam. These equations of equilibrium, which are nonlinear since the materials in the structure have nonlinear stress-strain relationships, were written by summing forces in the horizontal direction and summing moments about the centroid of the tendon on the free body diagram shown in Fig. 4. These equations appear in functional form below.

$$\Sigma F_x = 0 = F(\epsilon_b, \epsilon_t) - F_t \tag{3}$$

$$\Sigma M_t = 0 = M(\epsilon_b, \epsilon_t) - M_x \tag{4}$$

where ΣF_x = sum of forces in the horizontal direction

ΣM_t = sum of moments about the tendon centroid

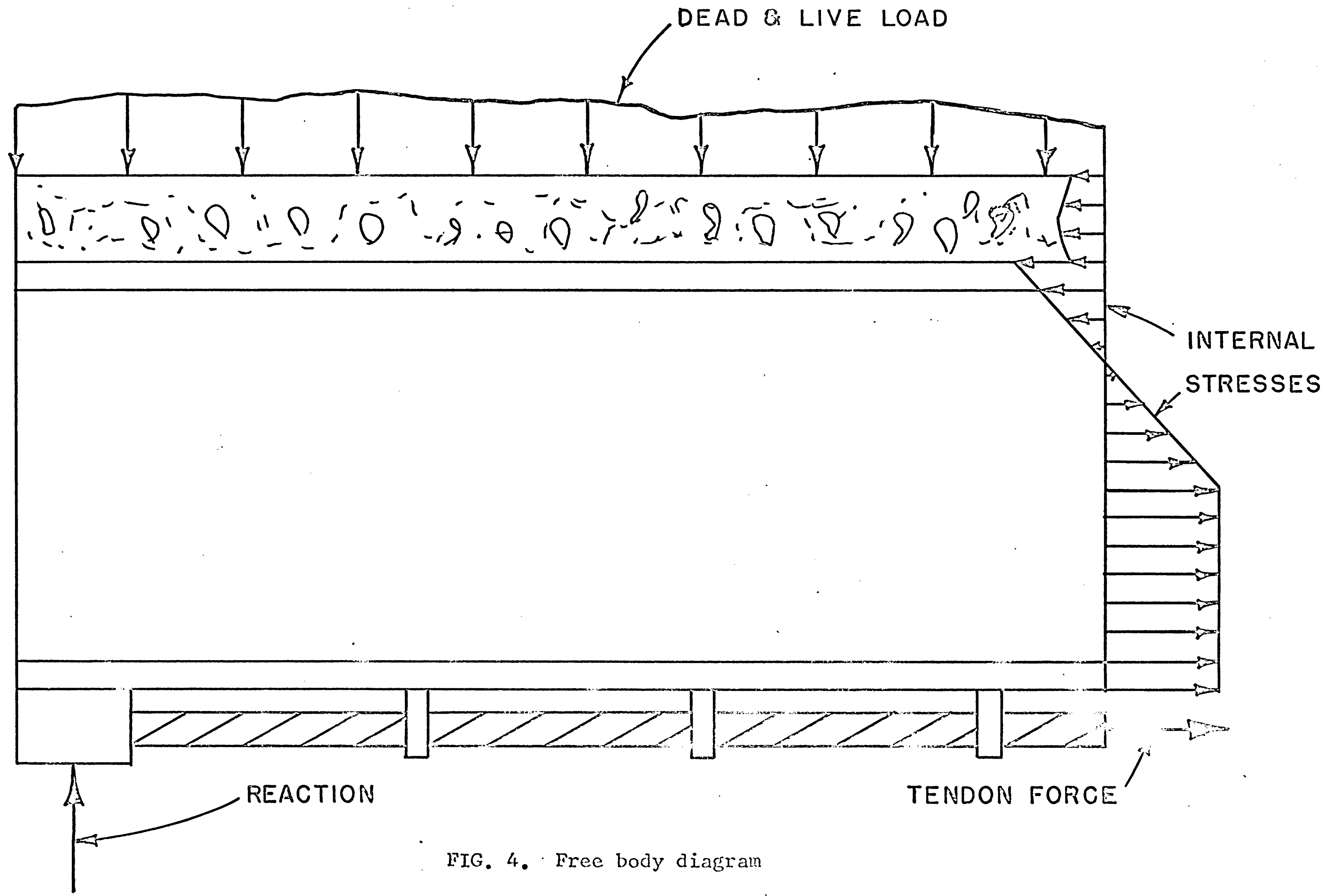

FIG. 4. Free body diagram

ϵ_b = strain at bottom of steel beam due to prestress, dead load, and live load

ϵ_t = strain at top of steel beam due to prestress, dead load, and live load

F_t = tendon force due to prestress, dead load, and live load

M_x = external moment at cross section due to dead and live loads

$F(\epsilon_b,\epsilon_t)$ = internal force at cross section

$M(\epsilon_b,\epsilon_t)$ = internal moment about tendon centroid at cross section

Since the distribution of strain across the cross section of the steel beam and concrete slab was assumed to be linear, the two strains ϵ_b and ϵ_t were used to specify the total strain distribution at a cross section of the prestressed composite beam. The strain distribution in the concrete at a cross section was found by subtracting the initial strain distribution from the total strain distribution, since the concrete slab only "knows about" the deformations produced by the live load.

The iterative method of tangents[11] for a single nonlinear equation was used to solve Eq. 3 for ϵ_t at midspan corresponding to an assumed value of the tendon force F_t and to the value of ϵ_b at midspan which was the quantity incremented until failure of the structure. Then Eq. 4 was used to find the external moment M_x at midspan, which was used in the load-moment relationship for the live load considered to find the live load on the beam. The iterative method of tangents[11] for two simultaneous non-linear equations was used to solve Eqs. 3 and 4 simultaneously for values of ϵ_b and ϵ_t corresponding to the assumed F_t and M_x values calculated from the applied load at a discrete number of equally spaced node points along half of the length of the beam, as the structure and loading was assumed to be symmetrical. The value of $F(\epsilon_b,\epsilon_t)$ was found by integration of the stress distribution, as found from the stress-strain relationships, across the cross section of the steel beam and concrete slab, and $M(\epsilon_b,\epsilon_t)$ was found by determining the first moment of these stresses about the tendon centroid. This integration was done in closed form by breaking the integrals into pieces at each change of width of the cross section and at each change in stress-strain function. The values of $\partial F(\epsilon_b,\epsilon_t)/\partial\epsilon_b$, $\partial F(\epsilon_b,\epsilon_t)/\partial\epsilon_t$, $\partial M(\epsilon_b,\epsilon_t)/\partial\epsilon_b$, and $\partial M(\epsilon_b,\epsilon_t)/\partial\epsilon_t$ needed for the method of tangents were found by differentiation of the expressions for $F(\epsilon_b,\epsilon_t)$ and $M(\epsilon_b,\epsilon_t)$ found above. The iterations were continued until the calculated corrections to the strains were less than some fractional tolerance of the corresponding strains for the preceding increment.

A method of successive approximations was used to find the value of tendon force F_t for each strain increment in the following manner. First a value of tendon force for the strain increment was assumed and the deformations along the beam length corresponding to this assumption were found as described above. The tendon force corresponding to these calculated beam deformations was found. Then from the assumed and calculated values a new assumption was made and the process repeated until the assumed and calculated values agreed within a specified tolerance.

Steps in the application of the method

The line of reasoning used in the computer program appears in the flow chart, Fig. 5. Each box in the flow chart is numbered, and a more detailed discussion of the computations in each box appears in the following correspondingly numbered steps.

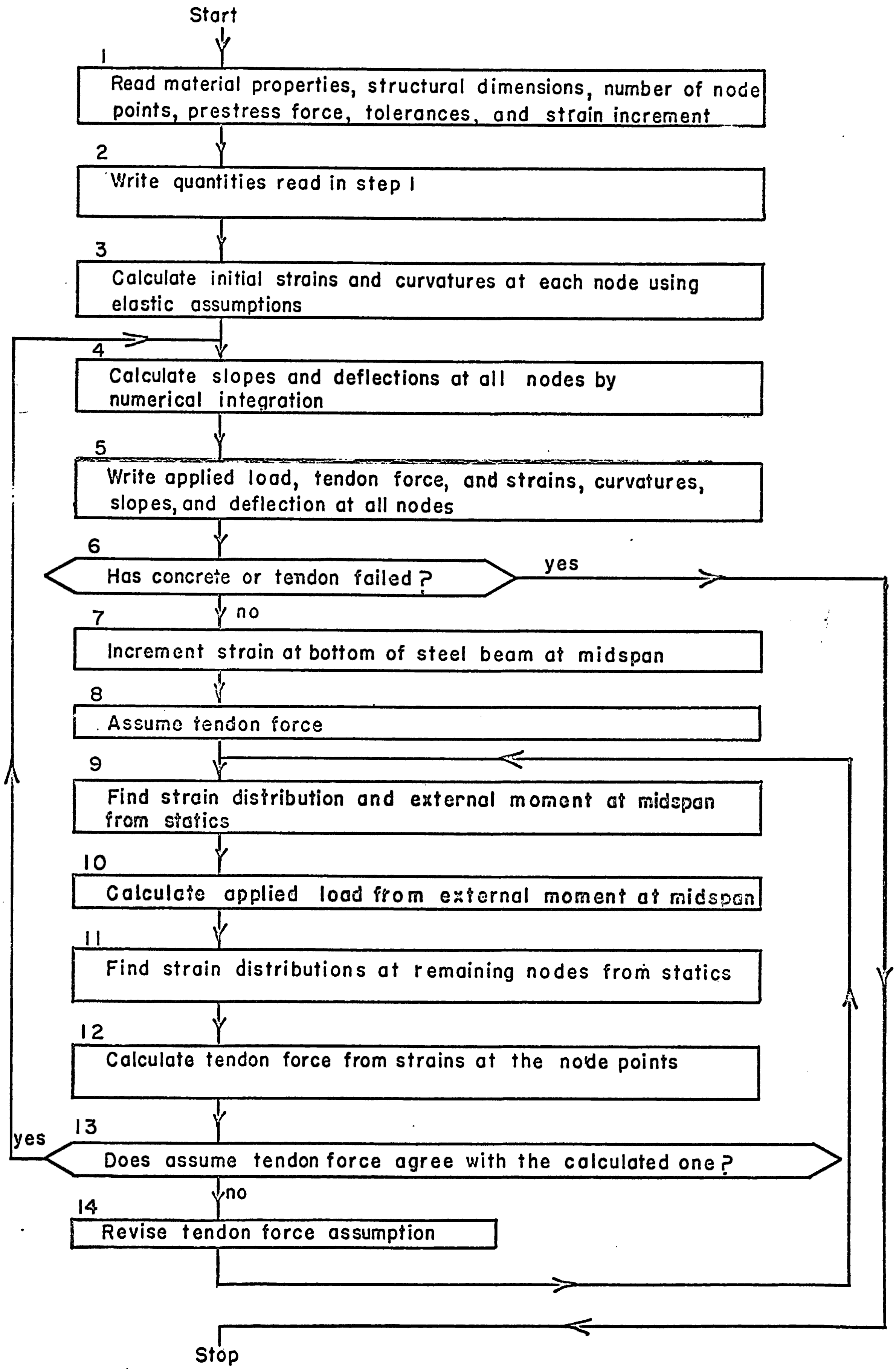

FIG. 5. Flow chart of computer program

1. Material properties, structural dimensions, prestress force, number of node points, tolerances for strains and tendon force, and increment by which the strain at the bottom of the steel beam at midspan is to be increased until the failure of the beam are read.
2. The quantities read in step 1 are written.
3. The initial strains and curvatures at each node point and the initial tendon force are found using the equations presented by Hoadley[4] based upon elastic assumptions. See Fig. 6 for the initial strain distribution at a typical cross section.
4. The slopes and deflections of all node points are calculated by numerical integration of the curvatures at the node points using a three-point quadrature formula.
5. The applied load, tendon force and strain, and strains, curvatures, slopes, and deflections at each node point are written. The first time this is done, the applied load is equal to zero and the other quantities are the initial conditions found in step 3.
6. The maximum concrete strains at all node points are compared with ϵ_u and the tendon force is compared with the ultimate tendon force. If either of these ultimate values has been exceeded, the structure has failed and the analysis is finished, and if not the analysis is continued in step 7.
7. The strain at the bottom of the steel beam ϵ_b at midspan is incremented by the amount specified in step 1.
8. A value for the tendon force is assumed. For the first strain increment the initial tendon force is assumed, for the second strain increment an assumption is obtained from straight line extrapolation, and for the third and successive strain increments parabolic extrapolation is used.

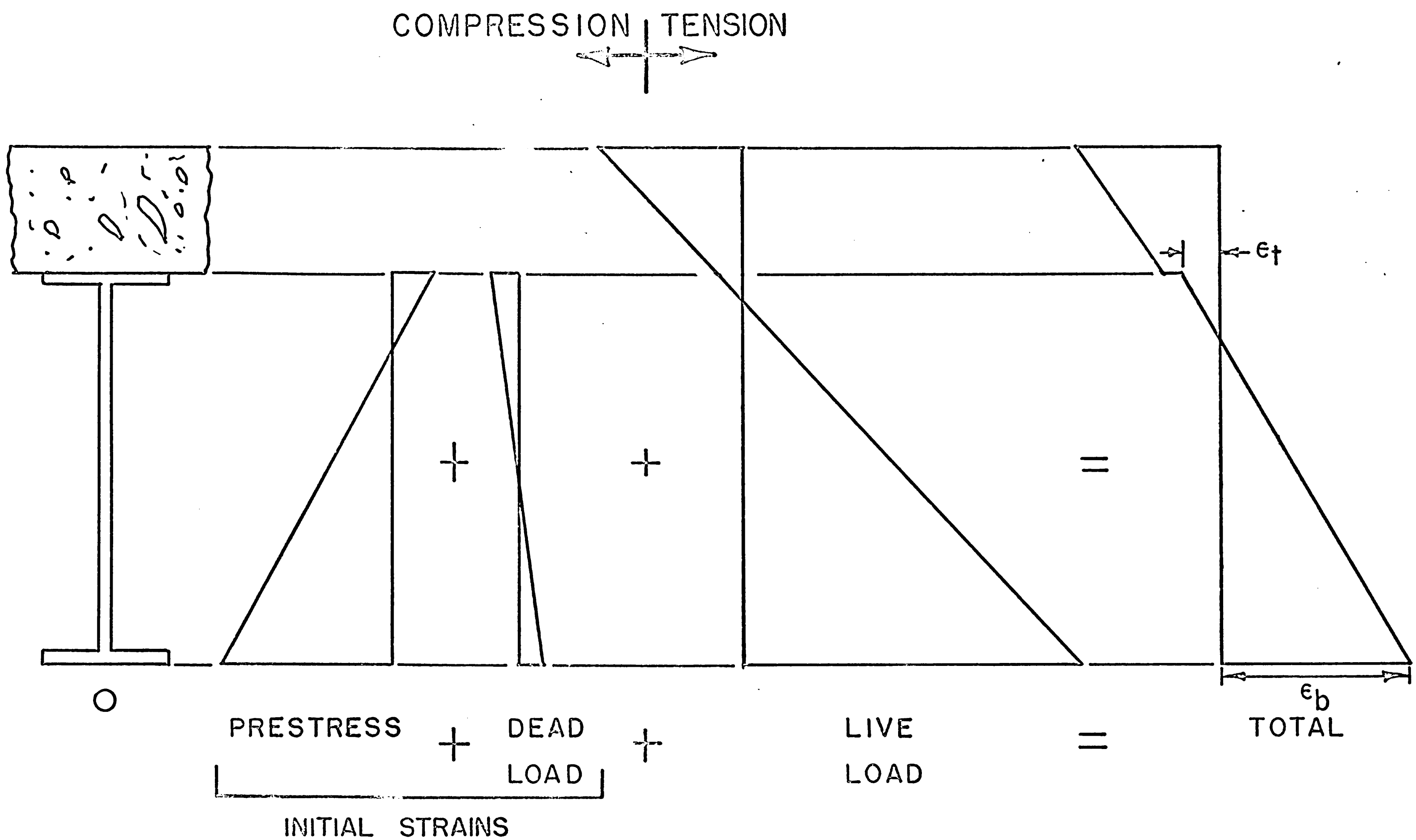

FIG. 6. Strain distributions at a typical cross section

9. The strain at the top of the steel beam ϵ_t at midspan is determined by solving Eq. 3 using the method of tangents. A starting value of ϵ_t for the first strain increment is calculated from equations presented by Hoadley[4], based upon elastic assumptions and the transformed section, and for successive strain increments from the same extrapolation procedures used in step 8 for F_t. The external moment M_x at midspan is found from Eq. 4.

10 The applied load on the beam is calculated from the external moment found in step 9.

11. The values of M_x at each node point are calculated, and the strains ϵ_b and ϵ_t at each node point are found by solving Eqs. 3 and 4 simultaneously using the method of tangents. Starting values for ϵ_b and ϵ_t are obtained as was done for ϵ_t in step 9. See Fig. 6 for the strain distribution at a typical cross section.

12. The tendon strain is calculated from the strains at the node points. The strain in the tendon is the same as the average strain in a fictitious "fiber" of the beam at the level of the tendon centroid and is obtained by numerically integrating the strains in this "fiber" at the node points along the length of the beam and dividing the result by the length of the tendon. Then the tendon force is calculated using the stress-strain relationship for the tendon.

13. The tendon force calculated in step 12 is compared with the tendon force assumed in step 8. If they agree within an amount less than the fractional tendon force tolerance specified in step 1 multiplied by the tendon force for the preceding strain increment, the analysis of the beam for this strain increment is finished, and the procedure is continued in step 4. If not the tendon force assumption is revised in step 14.

14. A new assumption for the tendon force is made. This is done for the second trial of each increment by assuming the average of the assumed and calculated values which are stored. Then for the third and successive trials, a new assumption is made, thinking of a plot of assumed tendon force vs. calculated tendon force, by finding the intersection of a straight line passing through two points representing the last two trials with the straight line on which the assumed tendon force equals the calculated tendon force. Then the analysis is continued in step 9.

The program described above for analyzing prestressed composite beams was modified to analyze conventional composite beams by removing from it all the statements concerned with the prestressing tendon. The average computer time required to analyze a structure with either of these programs, using a strain increment of 0.0003 and six node points, was about five minutes on the IBM 7040.

3. RESULTS

The method of analysis presented herein was used to study the structural behavior of thirty-one prestressed and conventional composite beams in the following categories:

(1) Beams of a configuration which might be found in a highway bridge

(2) Beams of a configuration which might be found in a building

(3) Beams for which experimental results are available

In all of the beams studied the dead load of the structure (weight of the concrete slab, steel beam, and tendon or cover plate) was assumed to be carried by the steel beam alone. All the beams studied failed by crushing of the concrete, not breaking of the tendon.

In the first two categories the tendon stress-strain curve shown in Fig. 3 was used for all prestressed beams, and the following material properties were used: concrete cylinder strength, $f_c' = 3000$ psi; ultimate concrete strain, $\epsilon_u = 0.0038$; yield stress of the steel beam, $f_y = 36{,}000$ psi; and modulus of elasticity of the steel beam, $E_s = 29 \times 10^6$ psi. For the third category the material properties used were those that the experimenter obtained from samples of the materials used in the test specimens.

For the first two categories allowable loads were determined which were used in the calculation of factors of safety. The allowable load was taken as the greatest load at which neither the steel nor concrete stress at midspan, the section of maximum live load moment, exceeded the allowable stress specified by the appropriate building code. The steel stress at the support in the beams which were highly prestressed exceeded the allowable steel stress or even the yield stress at a load less than the allowable load. Over the support the concrete is in tension, since there is no external moment at the support, and therefore takes no stress, and the steel beam must carry the stresses caused by the prestress force and the increase in the tendon force caused by live load. Thus if the steel beam is stressed to near or above its allowable stress by the prestress force, the increase in the tendon force may cause the steel stress at the support to exceed the allowable stress or even the yield stress at a load less than what is here defined, somewhat arbitrarily, as the allowable load. This point is discussed more fully later in this chapter.

Analytical results for the highway bridge beams

The basic configurations and loading of the prestressed and conventional composite highway bridge beams appear in Fig. 7(a). The live load consists of a concentrated load and a uniformly distributed load applied in the same ratio as the concentrated and distributed loads in the AASHO H20-S16-44 lane loading for flexure[12]. In the following results for the highway bridge beams, only the concentrated live load P lb. is given; let it be emphasized that the concentrated load is always accompanied by a uniformly distributed live load of 8P/2700 lb./in.

The design of composite highway bridge beams is covered by the AASHO code. The allowable stresses as specified by this code are for the concrete, $0.4f'_c = 1200$ psi, and for the steel beam, 20,000 psi[13]. The code also limits the deflection due to live load to 1/800 of the span length which corresponds to 1.18 in. for a 79 ft. span.

Table 1 for the prestressed composite highway bridge beams, designated PH1 through PH10, contains for each beam the slab depth, the number and

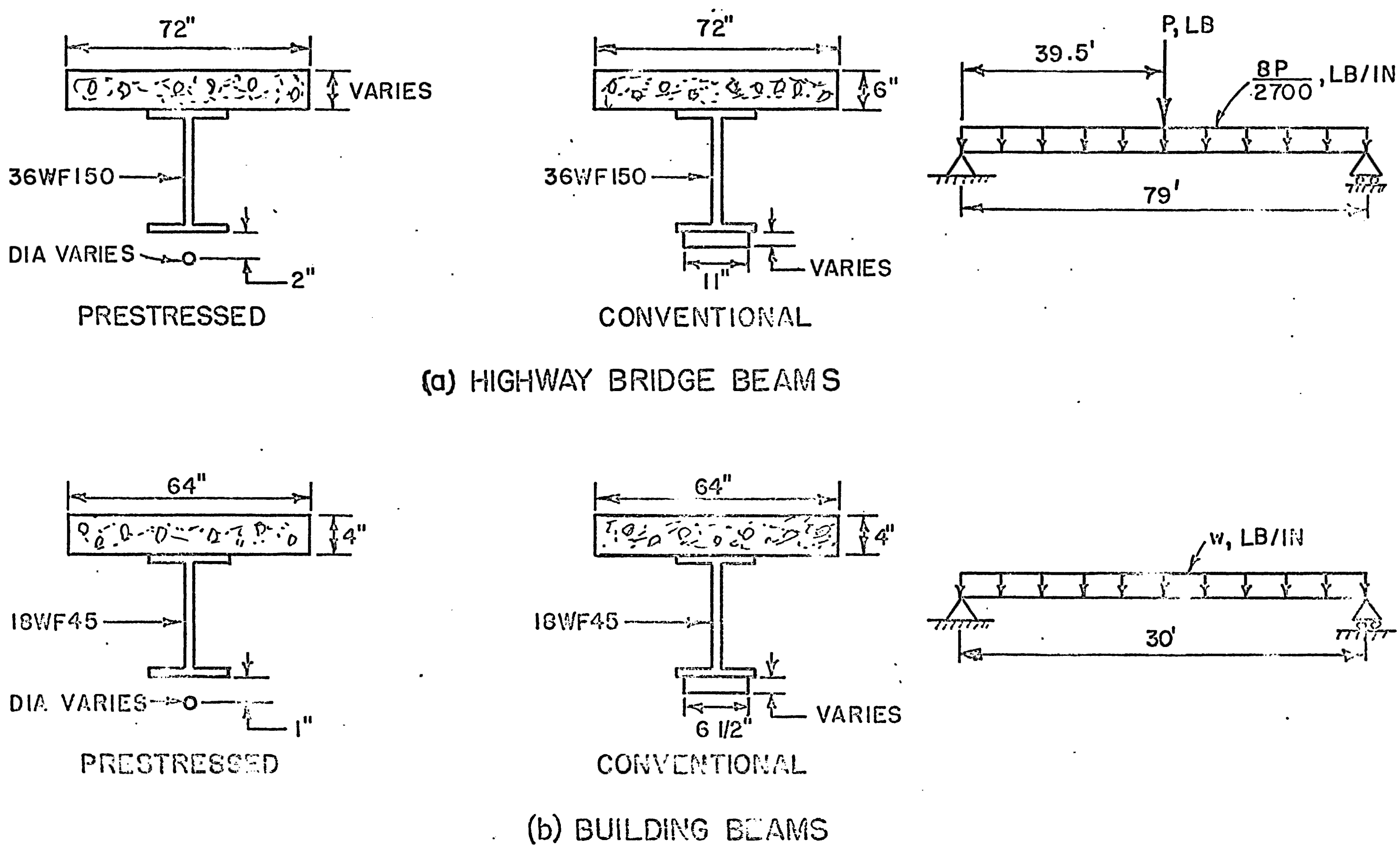

FIG. 7. Description of structures studied analytically

TABLE 1. Results for prestressed composite highway bridge beams

Beam no.	Slab depth, in.	Tendon, no.-dia., in.	Pre-stress force, kips	Max. steel stress due to pre-stress, ksi	Yield load,* lb.	Ulti-mate load,* lb.	Tendon force at failure, kips	% incr. in tendon force at failure	Yield F. S.	Ultimate F. S.
PH1	6	1-1 1/4	0	0	29280	48770	67.44	-----	2.73	4.55
PH2	6	1-1 1/4	100	6.302	35680	55280	166.6	56.5	1.96	3.04
PH3	6	1-1 11/16	200	12.60	44200	64830	315.6	49.0	1.66	2.44
PH4	6	2-1 1/2	300	18.91	54110	73470	457.2	43.7	1.96	2.66
PH5	6	3-1 9/16	500	31.51	71750	86140	696.1	12.1	2.56	3.07
PH6	3	1-1 11/16	200	12.60	45740	55460	271.7	30.9	2.32	2.81
PH7	4	1-1 11/16	200	12.60	44440	59410	283.2	35.4	1.98	2.65
PH8	5	1-1 11/16	200	12.60	44280	62620	299.9	42.4	1.77	2.51
PH9	6	1-1 1/4	50	3.151	31730	51970	116.5	105.	2.20	3.60
PH10	6	1-1 1/4	150	9.454	38030	57830	205.9	31.4	1.73	2.63

*Each tabulated load P is a concentrated live load which is accompanied by a uniformly distributed live load of 8P/2700 lb./in. in order to use a loading proportional to AASHO H20-S16-44 lane loading.

diameter of tendons, the prestress force, the maximum stress in the steel beam due to the prestressing, the yield load (load corresponding to the first yielding of the steel beam at midspan), the ultimate load (load corresponding to the crushing of the concrete slab), the tendon force at failure of the beam, the percent increase in the tendon force due to live load at the failure of the beam, the factor of safety with respect to yield (ratio of the yield load to the allowable load), and the factor of safety with respect to ultimate (ratio of the ultimate load to the allowable load). Table 2 for the conventional composite highway bridge beams, designated CH1 through CH4, gives for each beam the cover plate size, the yield load, the ultimate load, and the factors of safety with respect to yield and ultimate.

Detailed graphical results are presented for one typical prestressed beam, beam PH3, only. The load-strain curves for beam PH3 appear in Figs. 8 and 9. These curves and the deflected shapes for beam PH3 shown in Fig. 10 show that most of the deformation of the beam occurred at the midspan cross section. Thus the beam behaved as if a "plastic hinge" had formed at midspan.

Fig. 11 shows a plot of the increase in tendon force due to live load for beam PH3. This curve is linear up to the yield load, and then it flattens out, even though the tendon was still in the straight line portion of its stress-strain curve at failure of the beam. This is caused by the large deformations of the steel beam occurring after yielding which in turn cause a correspondingly large increase in the tendon force, since the tendon is attached to the ends of the steel beam and is restrained to remain a constant distance from it.

Figs. 12-15 summarize the behavior of all of the highway bridge beams

TABLE 2. Results for conventional composite highway bridge beams

Beam no.	Cover plate size, in. x in.	Yield load,* lb.	Ultimate load,* lb.	Yield F. S.	Ultimate F. S.
CH1	none	27960	44470	2.10	3.35
CH2	$\frac{1}{2}$ x 11	37290	56500	2.28	3.45
CH3	1 x 11	47680	68440	2.12	3.04
CH4	$1\frac{1}{2}$ x 11	58300	79360	2.05	2.79

* Each tabulated load P is a concentrated live load which is accompanied by a uniformly distributed live load of 8P/2700 lb./in. in order to use a loading proportional to AASHO H20-S16-44 lane loading.

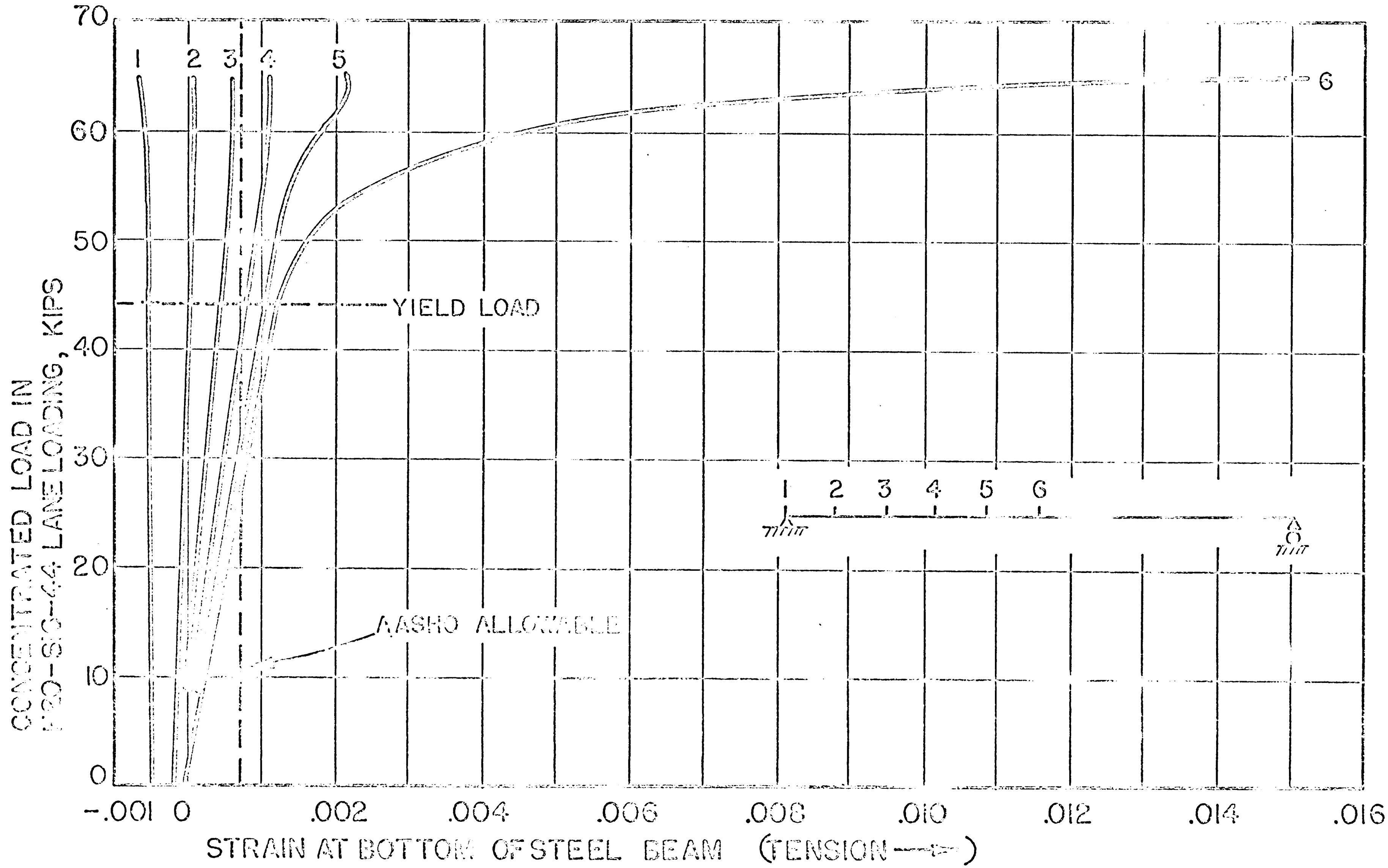

FIG. 8. Load vs. steel strain curves for beam PH3

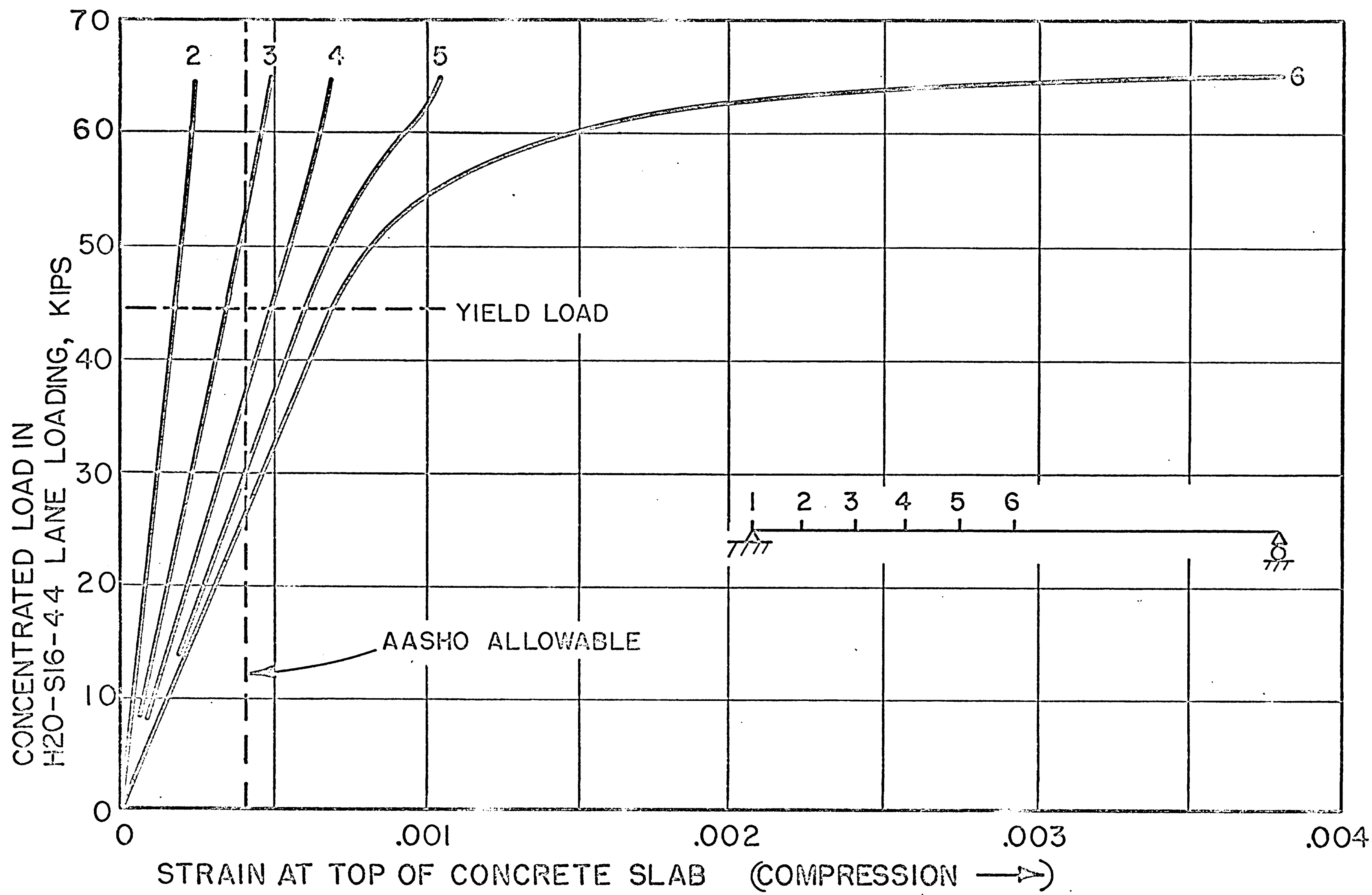

FIG. 9. Load vs. concrete strain curves for beam PH3

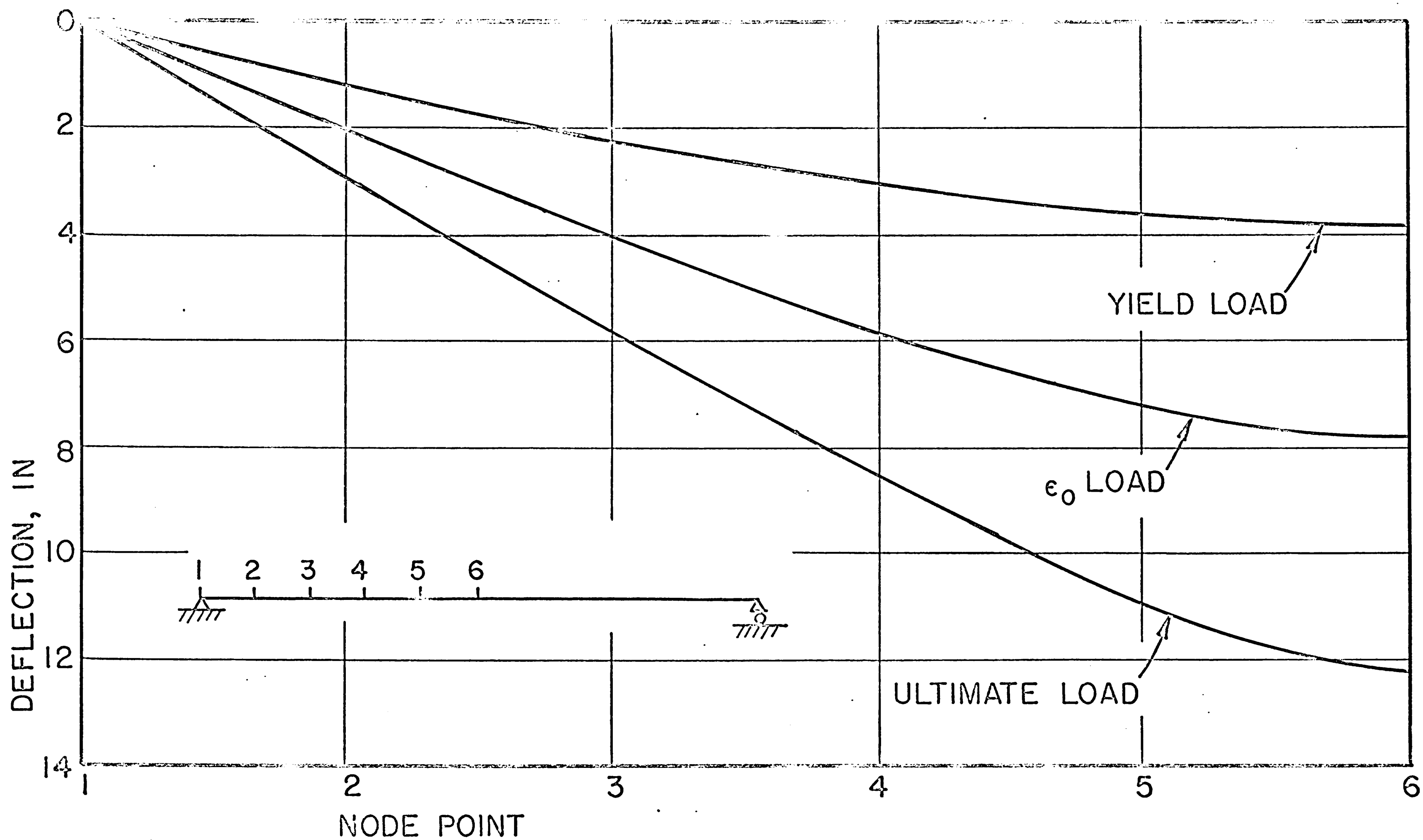

FIG. 10. Deflected shapes for beam PH3

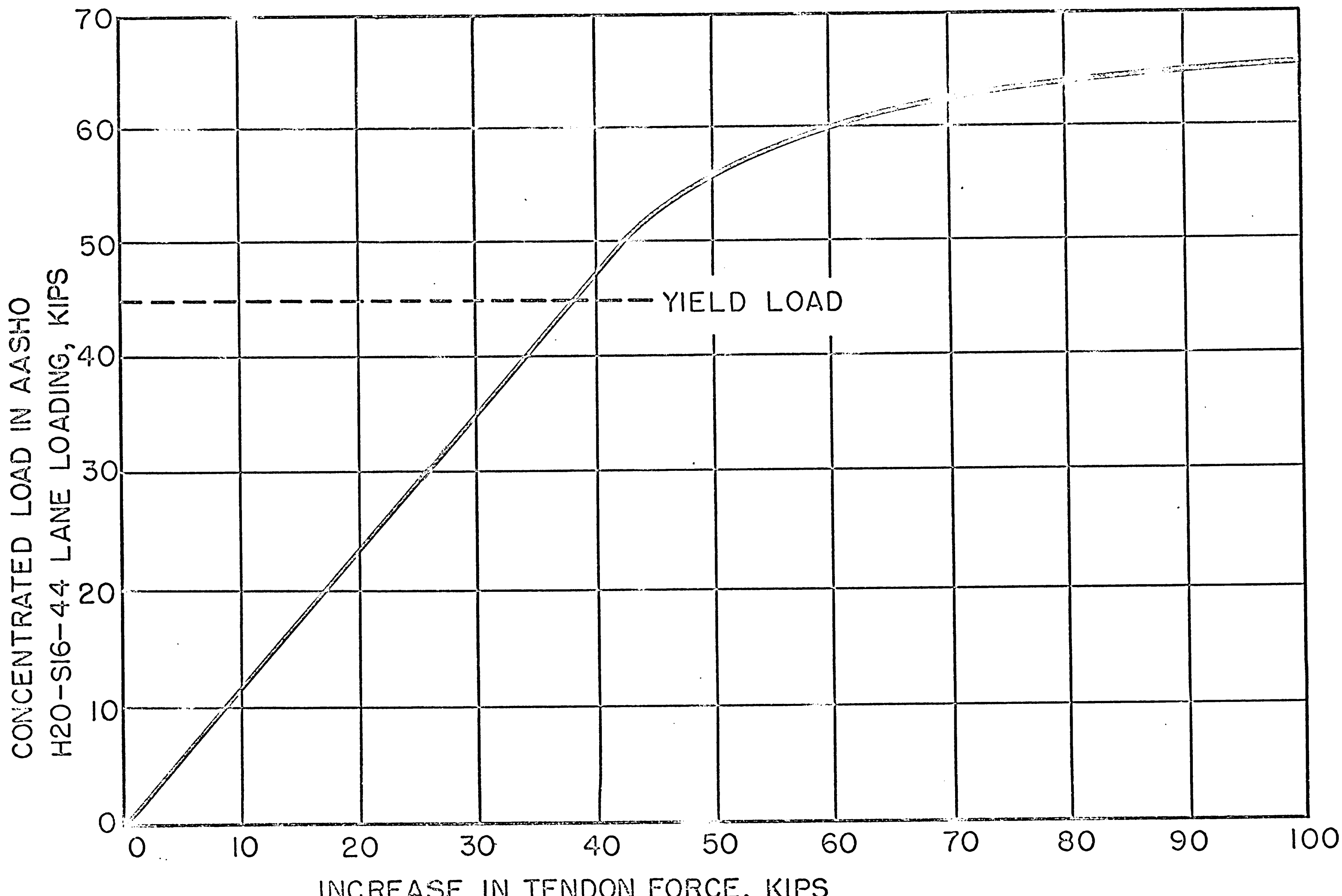

FIG. 11. Load vs. increase in tendon force curve for beam PH3

studied. These figures show curves of load vs. deflection at midspan with points corresponding to various stress and deformation conditions marked on each curve and corresponding points joined by a dotted line. The line marked "b-b" joins points corresponding to the load at which the steel stress at midspan equals the allowable steel stress. The line marked "c-c" joins points corresponding to the load at which the concrete stress at midspan equals the allowable concrete stress. The line marked "d-d" joins points corresponding to the load at which the deflection of the beam due to live load equals the AASHO allowable live load deflection. The line marked "o-o" joins points corresponding to the load at which the concrete strain at midspan equals ϵ_o. The line marked "y-y" joins points corresponding to the load at which the steel stress at midspan equals the yield stress. The point marked "s" corresponds to the load at which the steel stress at the support equals the yield stress. The curves are all stopped at the load corresponding to the crushing of the concrete.

The effect of variation of prestress force and tendon size is seen from the load-deflection curves shown in Fig. 12 for beams PH1 through PH5. The prestress force used in each of these beams was nearly equal to the recommended working load for the tendon. The slopes of lines "b-b" and "y-y" and a line passing through the end points of the curves show that increasing the prestress force and tendon size greatly increases the load that produces the allowable steel stress at midspan, the yield load, and the ultimate load. The slopes of lines "c-c" and "d-d" show that increasing the prestress force and tendon size only slightly increases the load that produces the allowable concrete stress at midspan and only slightly decreases the live load deflection. Beam PH5 yielded over the support at a load of 22.75 kips in the manner described above.

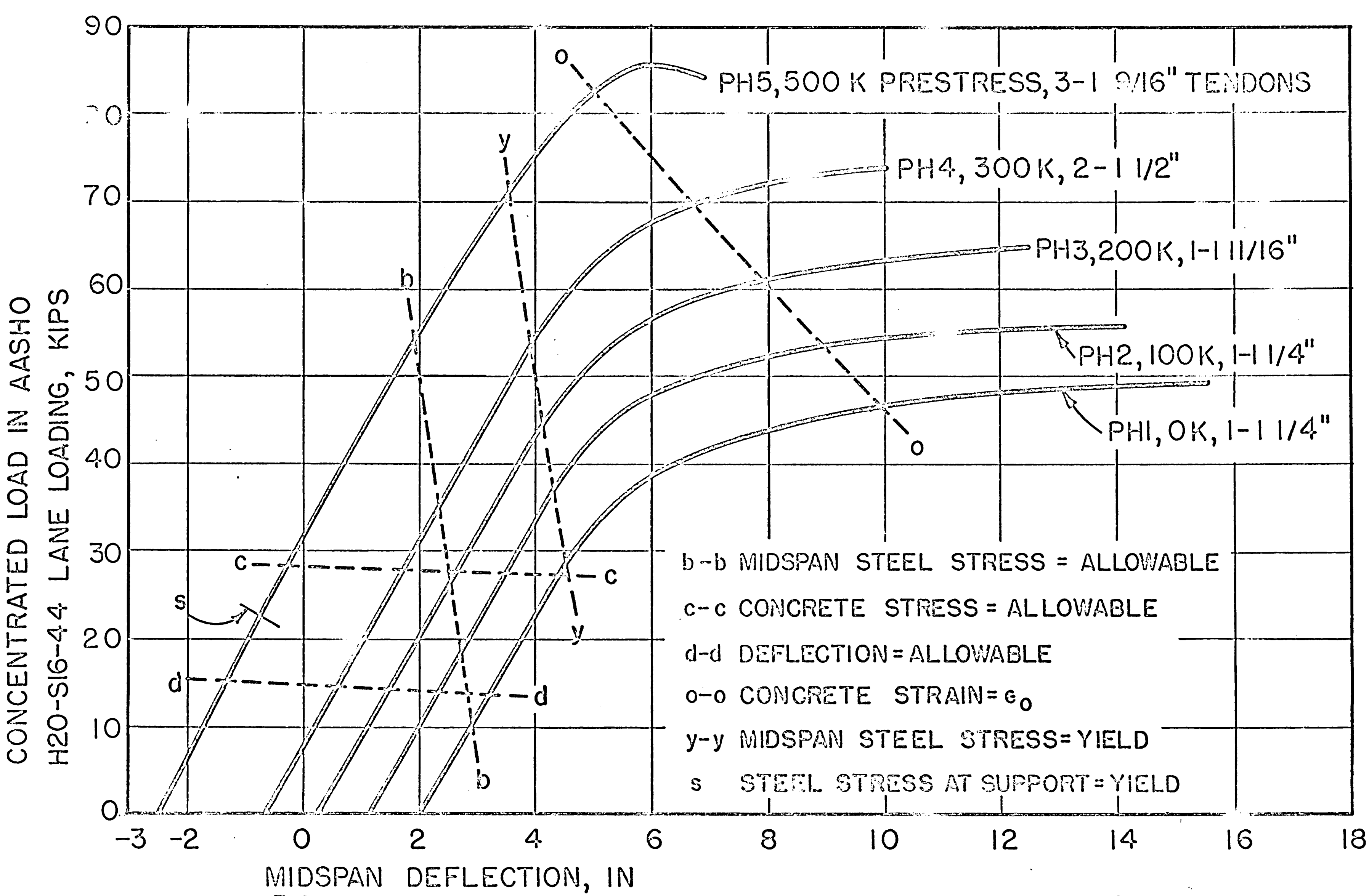

FIG. 12. Effect of variation of prestress and tendon for highway bridge beams

The effect of variation of the cover plate size for conventional composite highway bridge beams is seen in Fig. 13, the load-deflection curves for beams CH1 through CH4. These curves show that increasing the cover plate size greatly increases the load producing the allowable steel stress at midspan, the yield load, and the ultimate load. Unlike the effect of increasing the prestress force and tendon size, increasing the size of the cover plate does significantly reduce the live load deflection and does increase the load producing the allowable concrete stress at midspan.

The effect of increasing the prestress force on beams with the same tendon is seen from Fig. 14, the load-deflection curves for beams PH1, PH2, PH9, and PH10. Beam PH10 was the only beam studied for which the prestress force exceeded the recommended design load for the tendon used. The curves show that any increase in the prestress force increases the yield and ultimate loads and the load producing the allowable stress in the steel beam at midspan. They also show that, if the tendon size is not increased with an increase in prestress force, the load producing the allowable concrete stress and the live load deflection are unchanged.

The effect of variation of the slab thickness on prestressed composite beams with the same tendon and prestress force is seen in Fig. 15. the load-deflection curves for beams PH3, PH6, PH7, and PH8. Increasing the slab thickness increases the ultimate load, but, as is shown by the figure and Table 1, slightly reduces the yield load, since the increased dead load reduces the effect of the prestressing. The curves all cross at a load of about 30 kips, since increasing the slab thickness increases the stiffness, but also increases the dead load and the initial deflection.

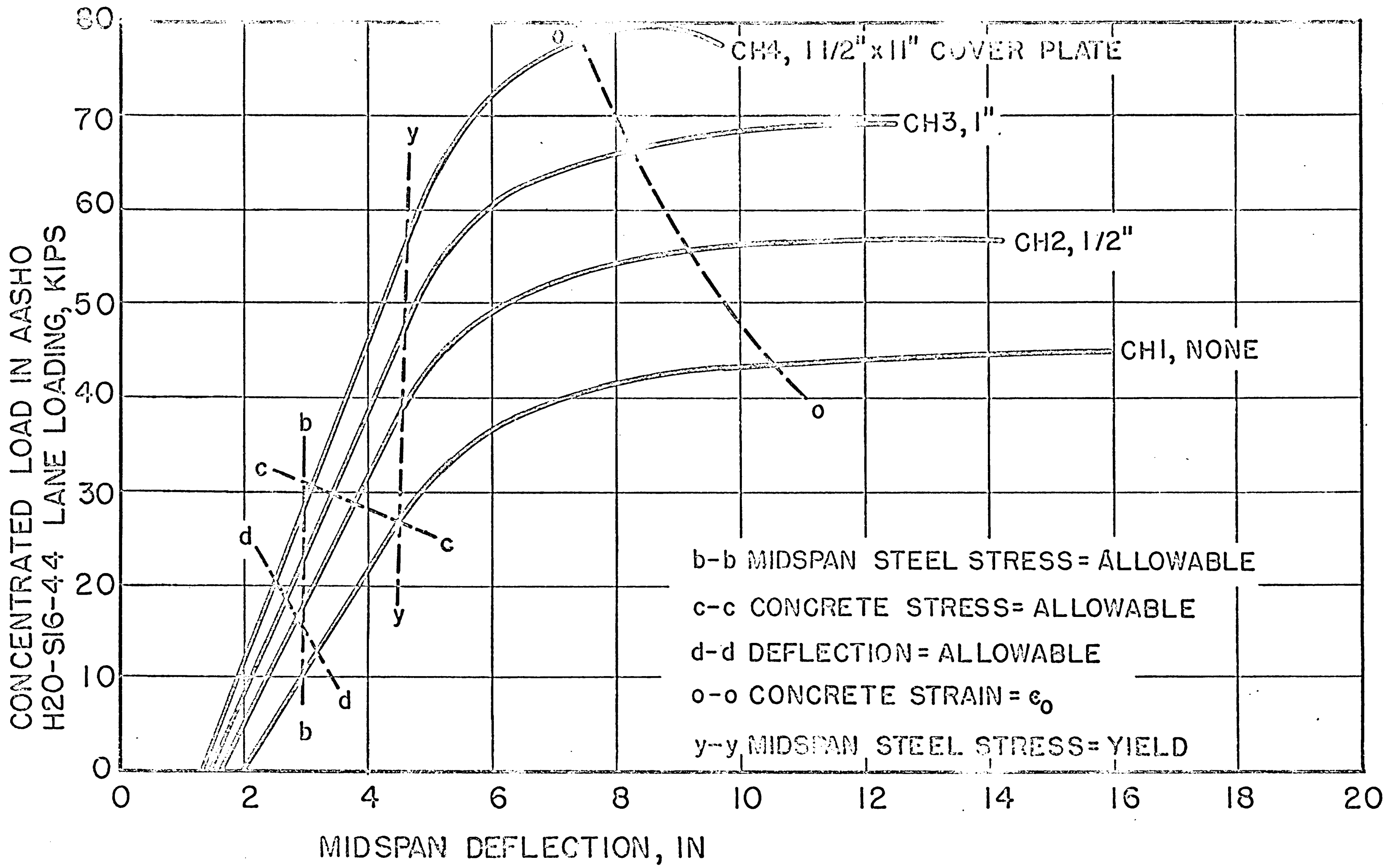

FIG. 13. Effect of variation of cover plate size for highway bridge beams

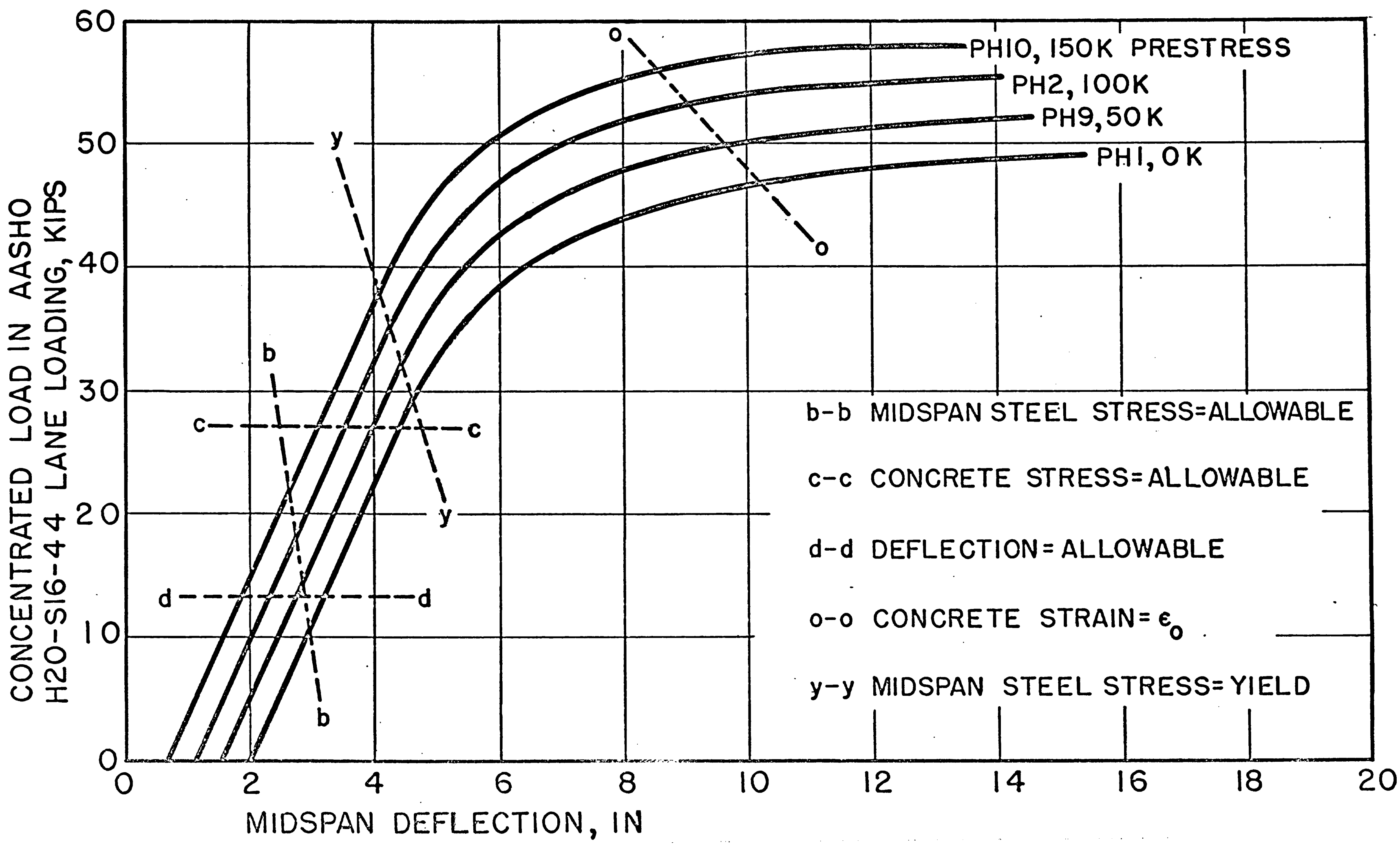

FIG. 14. Effect of variation of prestress for highway bridge beams

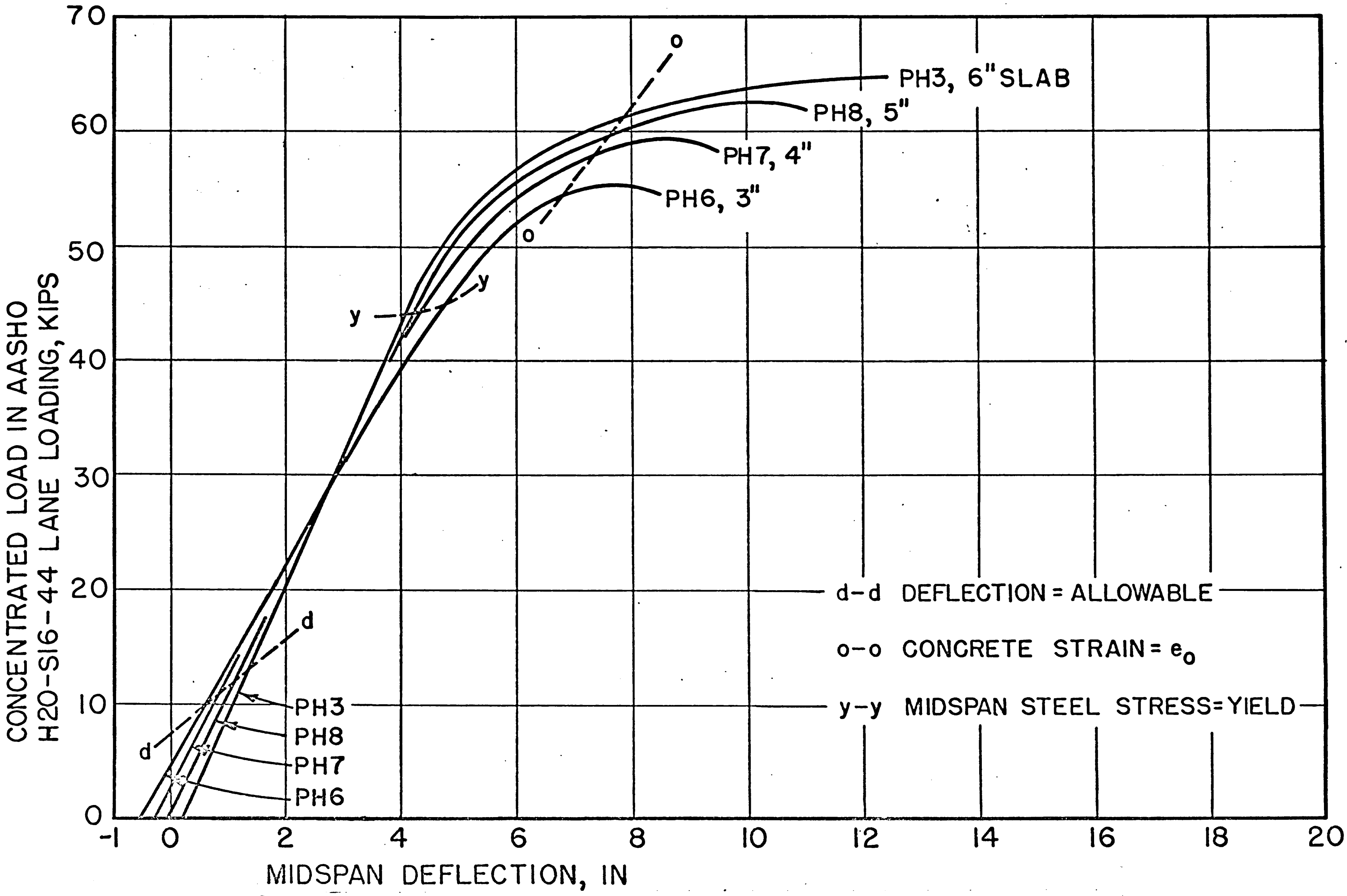

FIG. 15. Effect of variation of slab thickness for highway bridge beams

Analytical results for the building beams

The basic configuration and loading of the building beams studied appears in Fig. 7(b). The building beams were loaded with uniformly distributed live load.

The results for the same quantities appearing in Table 1 for the prestressed composite highway bridge beams appear in Table 3 for the prestressed composite building beams, designated PB1 through PB7, and the results for the same quantities appearing in Table 2 for the conventional composite highway bridge beams appear in Table 4 for the conventional composite building beams, designated CB1 through CB4.

The design of composite building beams is covered by the AISC[14] and ACI[15] codes. The allowable stresses for the building beams were taken as $0.66f_y$ = 24,000 psi for the steel beam as specified by the AISC code and $0.45f'_c$ = 1350 psi for the concrete slab as specified by the ACI code. The allowable live load deflection was taken as 1/360 of the span corresponding to 1 in. for a 30 ft. span as specified by the AISC code for beams and girders supporting plastered ceilings.

The graphical results for the building beams are presented in two load vs. deflection at midspan curves marked with dotted lines as described in the highway bridge beam results.

The effect of the variation of prestress and tendon size appears in Fig. 16. the load-deflection curves for beams PB1, PB3, PB5, and PB7. These curves show, as did Fig. 12, that increasing the prestress force and tendon size greatly increases the yield and ultimate loads and the load producing the allowable steel stress at midspan, slightly increases the load producing the allowable concrete stress at midspan, and slightly decreases the live load deflection. Beam PB7 yielded over the support at

TABLE 3. Results for prestressed composite building beams

Beam no.	Slab depth, in.	Tendon, no.-dia., in.	Pre-stress force, kips	Max. steel stress due to pre-stress, ksi	Yield load, lb./in.	Ulti-mate load, lb./in.	Tendon force at failure, kips	% incr. in tendon force at failure	Yield F. S.	Ultimate F. S.
PB1	4	1-.6	0	0	203.6	329.3	23.12	-----	1.57	2.55
PB2	4	1-.6	25	5.093	243.1	356.6	46.09	81.3	1.48	2.17
PB3	4	1-.835	50	10.19	282.2	404.8	86.80	69.2	1.38	1.98
PB4	4	1-1	75	15.28	321.7	447.7	123.1	60.1	1.31	1.83
PB5	4	1-1 1/4	100	20.37	379.5	509.5	175.7	70.7	1.52	2.04
PB6	4	1-1 3/8	125	25.47	416.3	548.4	209.1	63.0	1.66	2.19
PB7	4	1-1 1/2	150	30.56	466.1	56[illegible].5	218.8	42.2	1.84	2.21

TABLE 4. Results for conventional composite building beams

Beam no.	Cover plate size, in. x in.	Yield load, lb./in.	Ultimate load, lb./in.	Yield F. S.	Ultimate F. S.
CB1	none	195.9	302.6	1.56	2.41
CB2	$\frac{1}{2} \times 6\frac{1}{2}$	327.3	435.2	1.55	2.06
CB3	$1 \times 6\frac{1}{2}$	445.3	570.4	1.56	2.00
CB4	$1\frac{1}{2} \times 6\frac{1}{2}$	573.9	707.1	1.76	2.17

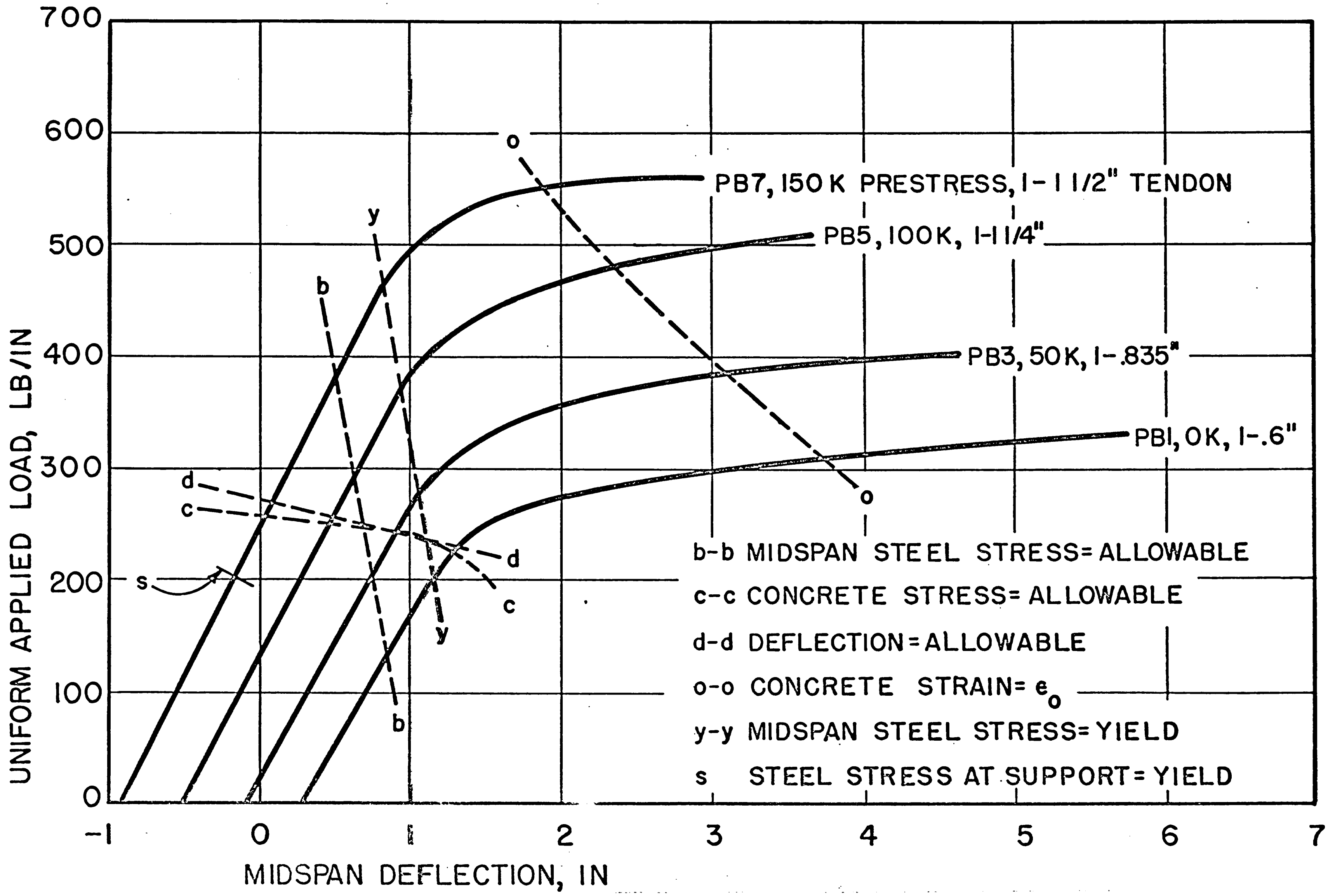

FIG. 16. Effect of variation of prestress and tendon for building beams

a load of 206.1 lb./in. in the manner previously described.

The effect of the variation of coverplate size on conventional composite building beams appears in Fig. 17, the load-deflection curves for beams CB1 through CB4. These curves show, as did Fig. 13, that increasing the cover plate size greatly increases the yield and ultimate loads and the load producing the allowable steel stress at midspan, and that increasing the cover plate size increases the load producing the allowable concrete stress at midspan and decreases the live load deflection much more than increasing the prestress force and tendon size does.

Comparison of analytical results with available experimental results

The computer program was used to analyze several beams for which experimental results from other investigators were available, in order to check the validity of all the analytical results obtained. The configuration and loading for each of these beams appears in Fig. 18.

Fig. 19 shows experimental and analytical load-deflection results for beam B24W of the series of tests made by I. M. Viest, C. P. Siess, H. H. Appleton, and N. M. Newmark[16] at the University of Illinois. Fig. 20 shows experimental and analytical load-deflection results for beam B1-T1 in the series of tests conducted at Lehigh University and reported by C. Culver and R. Coston[17]. The agreement between experimental and analytical results for both these beams is quite good.

Fig. 21 and 22 show experimental and analytical results for moment-deflection for beams 11, 41A, and 41B in the series of tests conducted by A. A. Toprac[18] at the University of Texas. Beams 41A and 41B were identical except for the concrete strengths which were 4770 psi for beam 41A and 3640 psi for beam 41B. The agreement between experimental and analytical results is not as good as it is for the Illinois and Lehigh

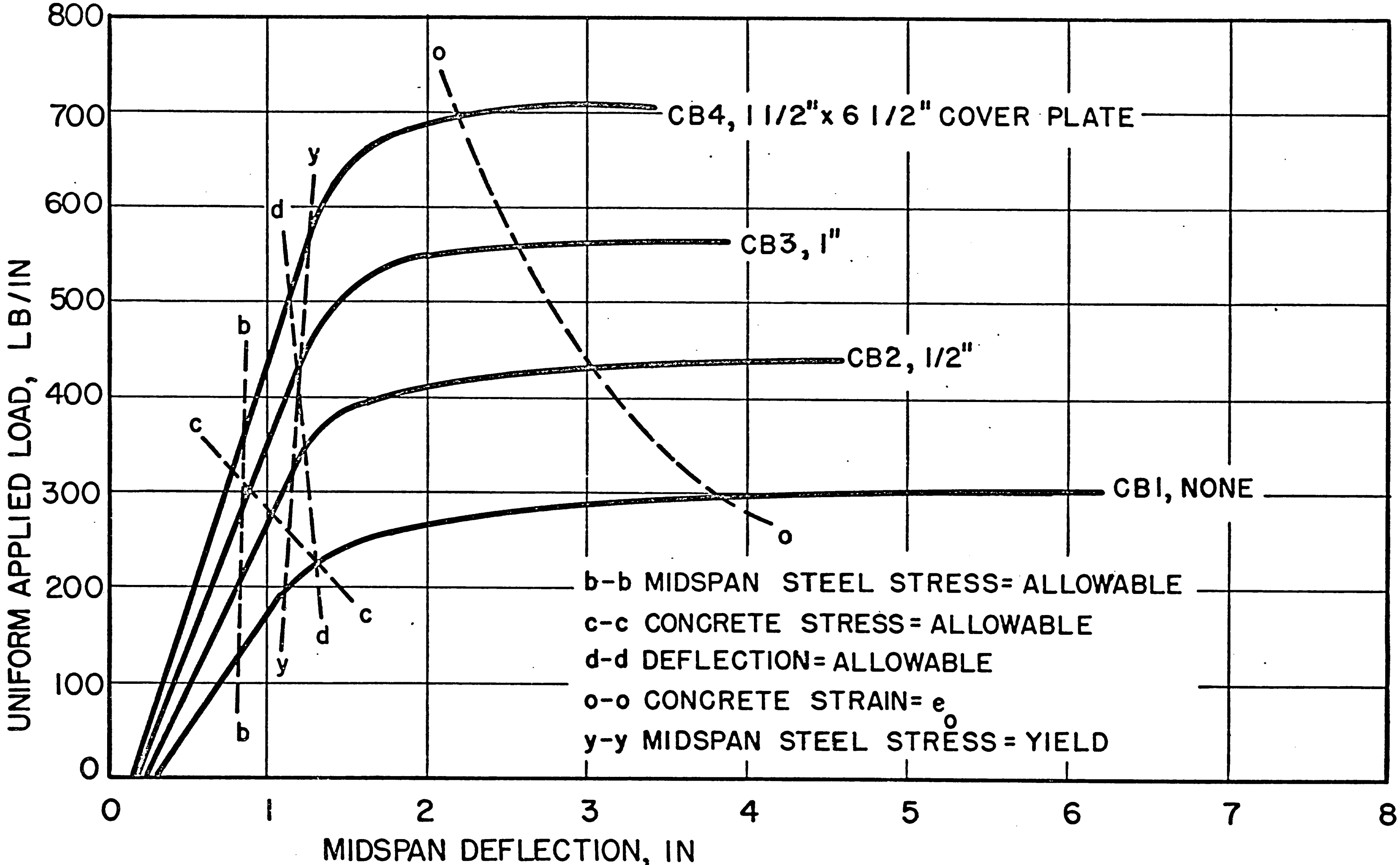

FIG. 17. Effect of variation of cover plate size for building beams

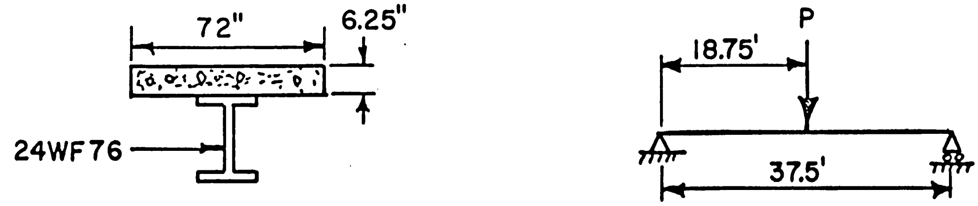

(a) ILLINOIS BEAM B24W

(b) LEHIGH BEAM B1

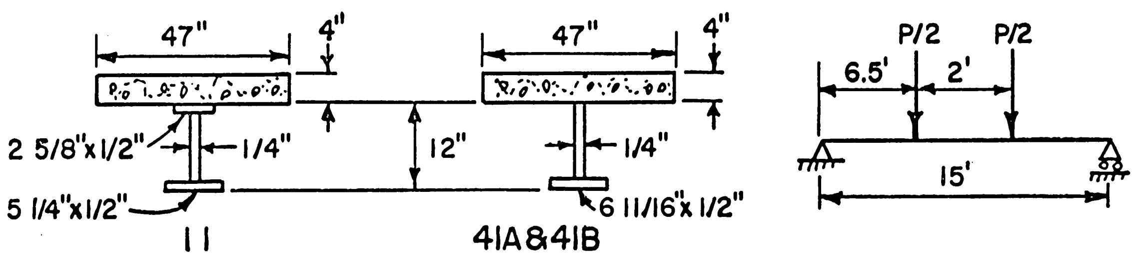

(c) TEXAS BEAMS

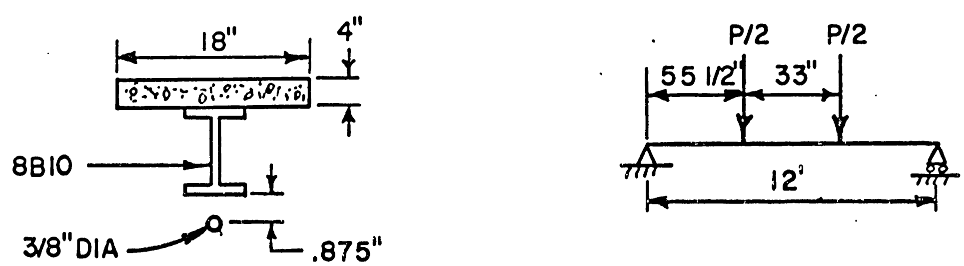

(d) RICE BEAMS

FIG. 18. Descriptions of structures for which experimental results are available

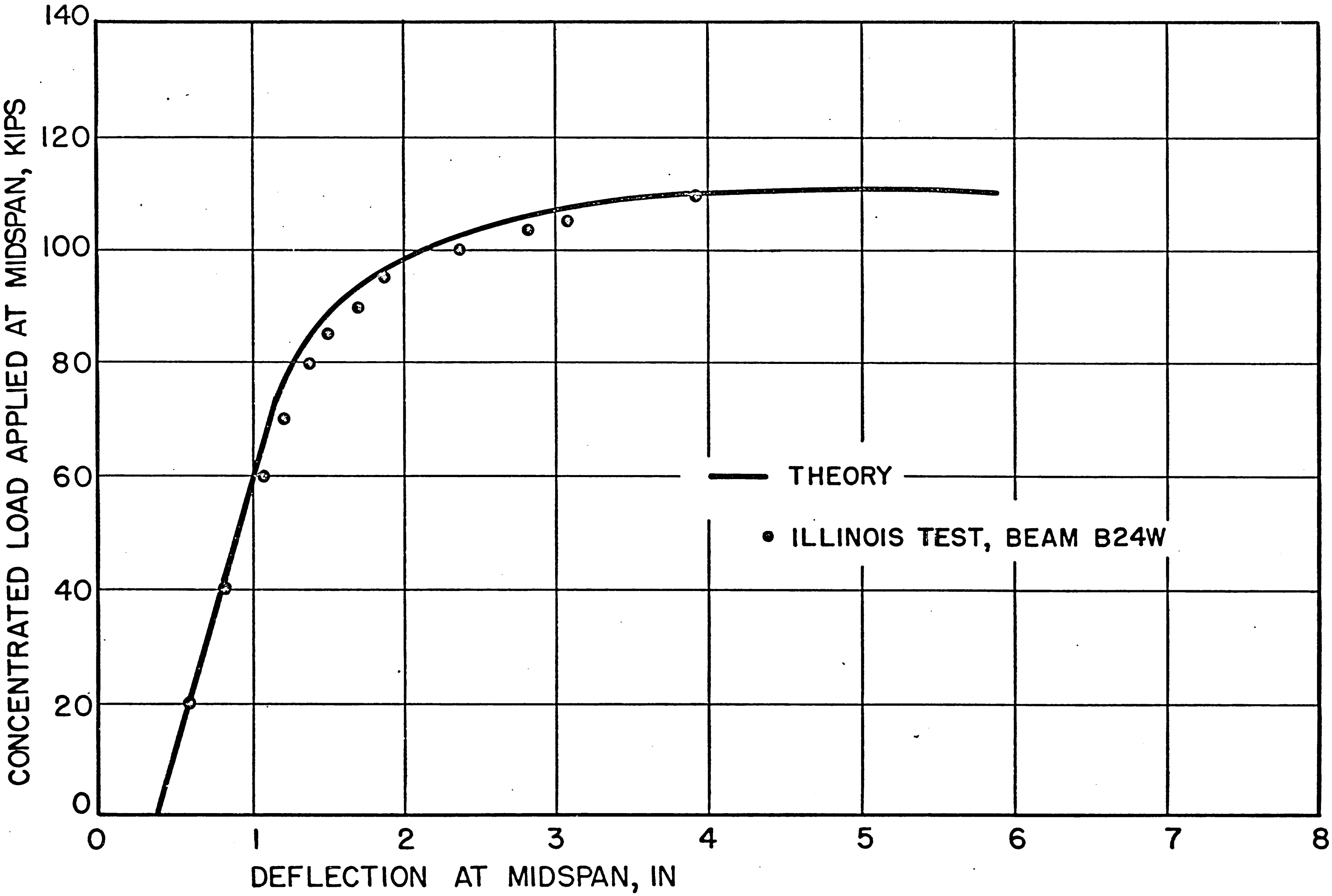

FIG. 19. Analytical and experimental results for Illinois beam B24W

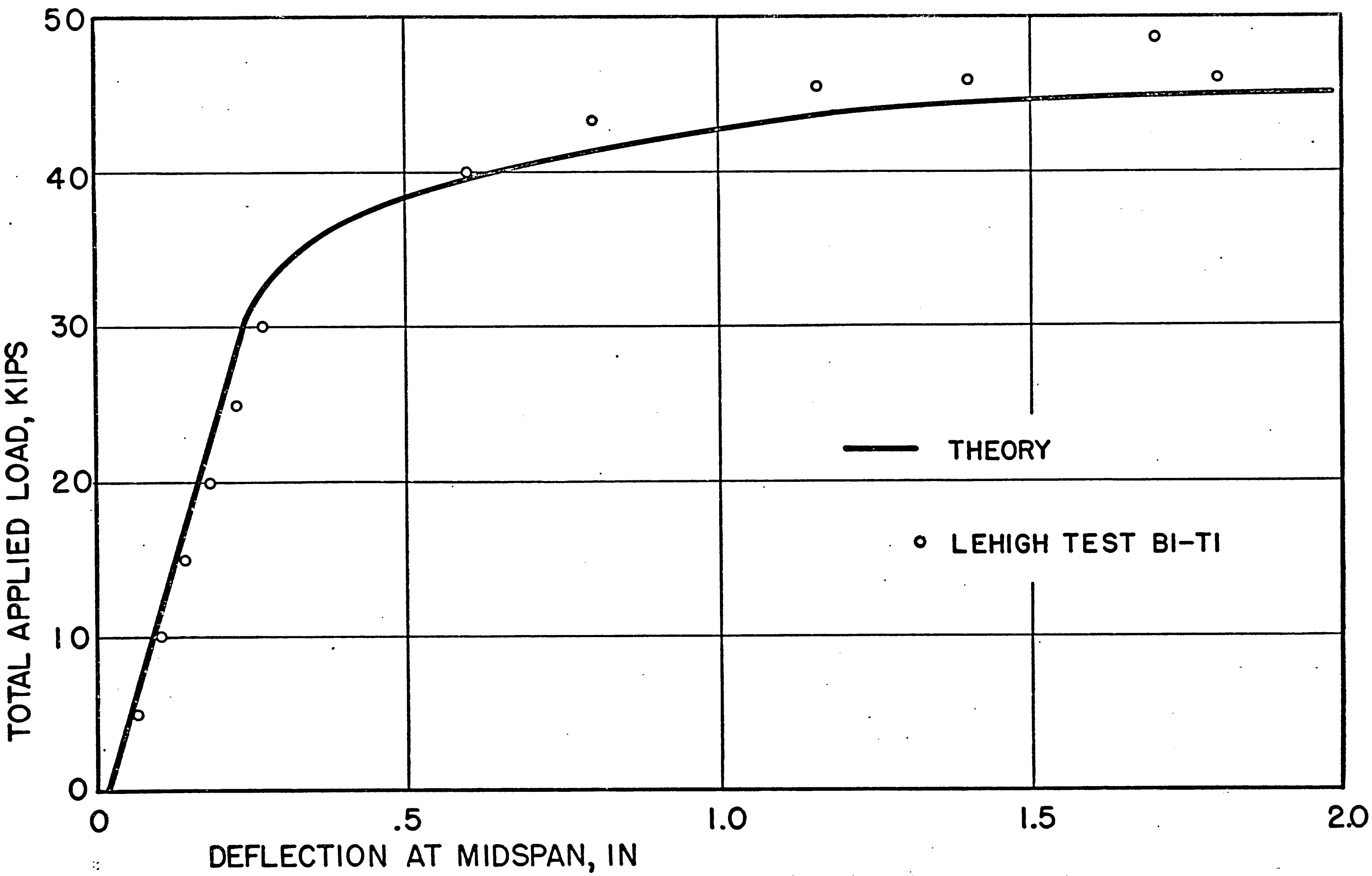

FIG. 20. Analytical and experimental results for Lehigh beam B1-T1

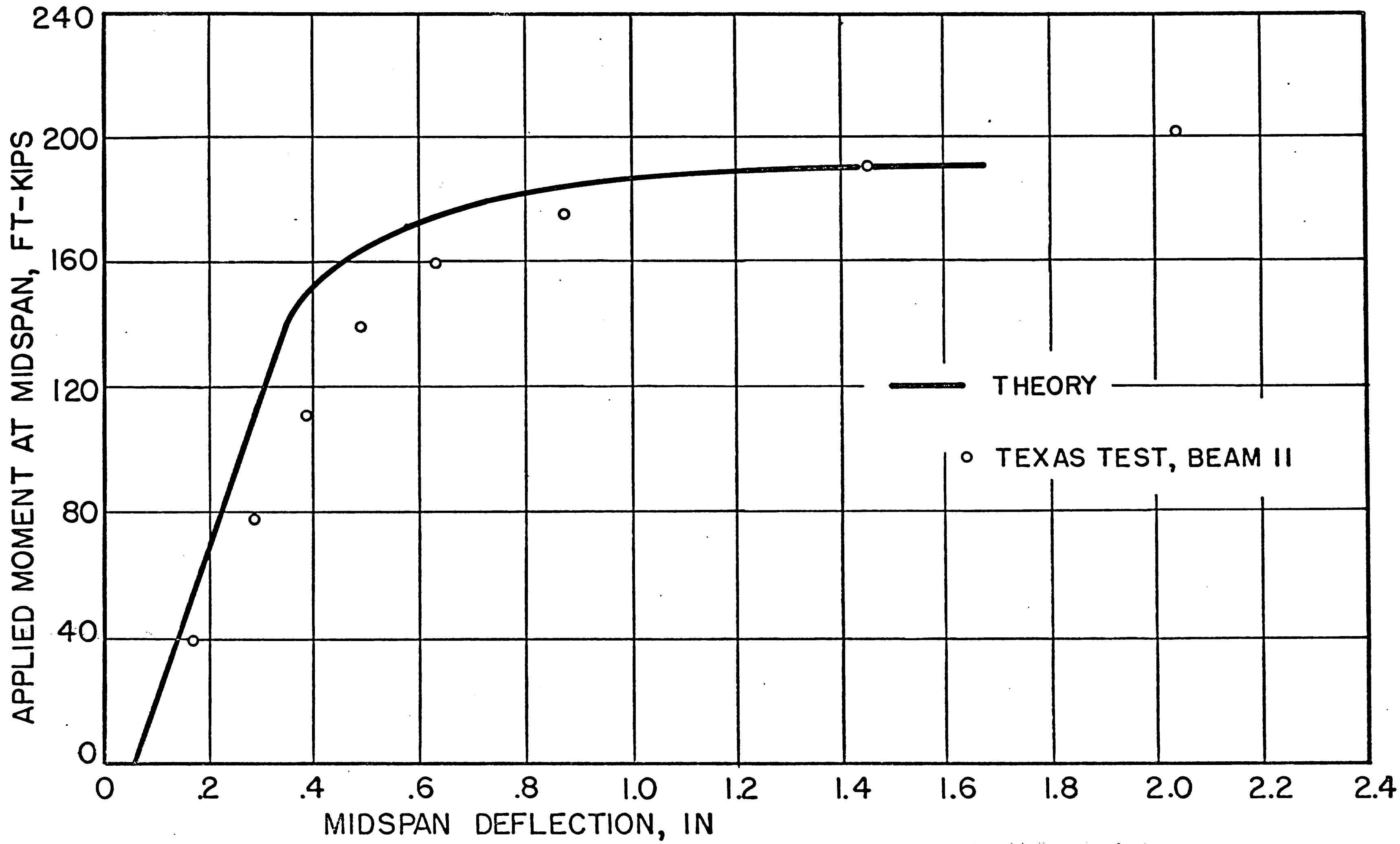

FIG. 21. Analytical and experimental results for Texas beam 11

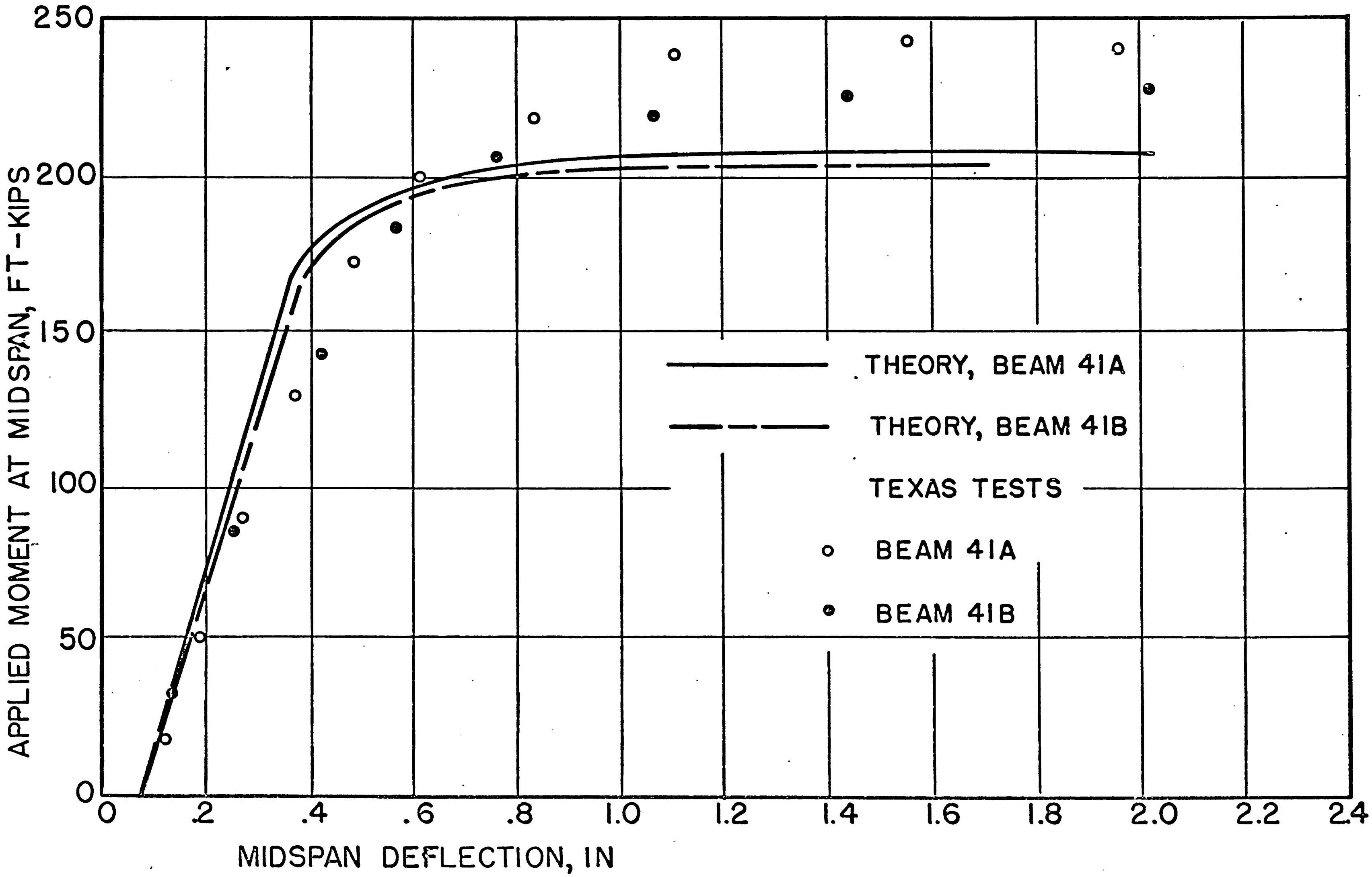

FIG. 22. Analytical and experimental results for Texas beams 41A and 41B

beams. The slopes of the analytical curves are greater in the elastic range than the slopes of the experimental points, and the experimental points lie above the theoretical curves in the inelastic range. Similar discrepancies were shown by Toprac between the experimental points and the slopes of curves based on elastic calculations, and the experimental points in the inelastic range were above the ultimate loads he calculated from rectangular stress blocks. The reason for these discrepancies is not known by the author nor was it given by Toprac. Possible explanations might be lack of complete interaction or a nonuniform distribution of strain across the width of the concrete slab, both of which violate the assumptions used in the analysis. The concrete slab in the Texas beams had the largest width/span and width/depth ratios of the beams studied as shown in Table 5.

Figs. 23, 24, and 25 show experimental and analytical results for load vs. concrete strain, load vs. change in tendon force, and load vs. midspan deflection, respectively, for beams A, B, and C tested by J. C. Stras III[8] at Rice University in 1964. To the author's knowledge, these are the only experimental results available for prestressed composite beams. These beams were prestressed with a force of 8.5 kips. The agreement between experiment and analysis is quite good. The yielding of the steel beams at a value of load less than the theoretical yield load, as seen in Fig. 25, may have been caused by residual stresses in the steel beams. This same phenomenon was observed by P. R. Barnard[19] in the analytical and experimental moment-curvature relationships he obtained for composite beams.

TABLE 5. Width/span and width/depth ratios of the concrete slabs used in the beams for which experimental results are available

Beam	Width/span ratio	Width/depth ratio
Illinois	.160	11.5
Lehigh	.200	8.0
Texas	.261	11.75
Rice	.125	4.5
AASHO max. allowed ratios	.250	12.0
AISC max. allowed ratios	.250	16.0*

* This is not exactly correct, since the AISC code allows the slab width to be 16 times the thickness plus the flange width of the steel beam.

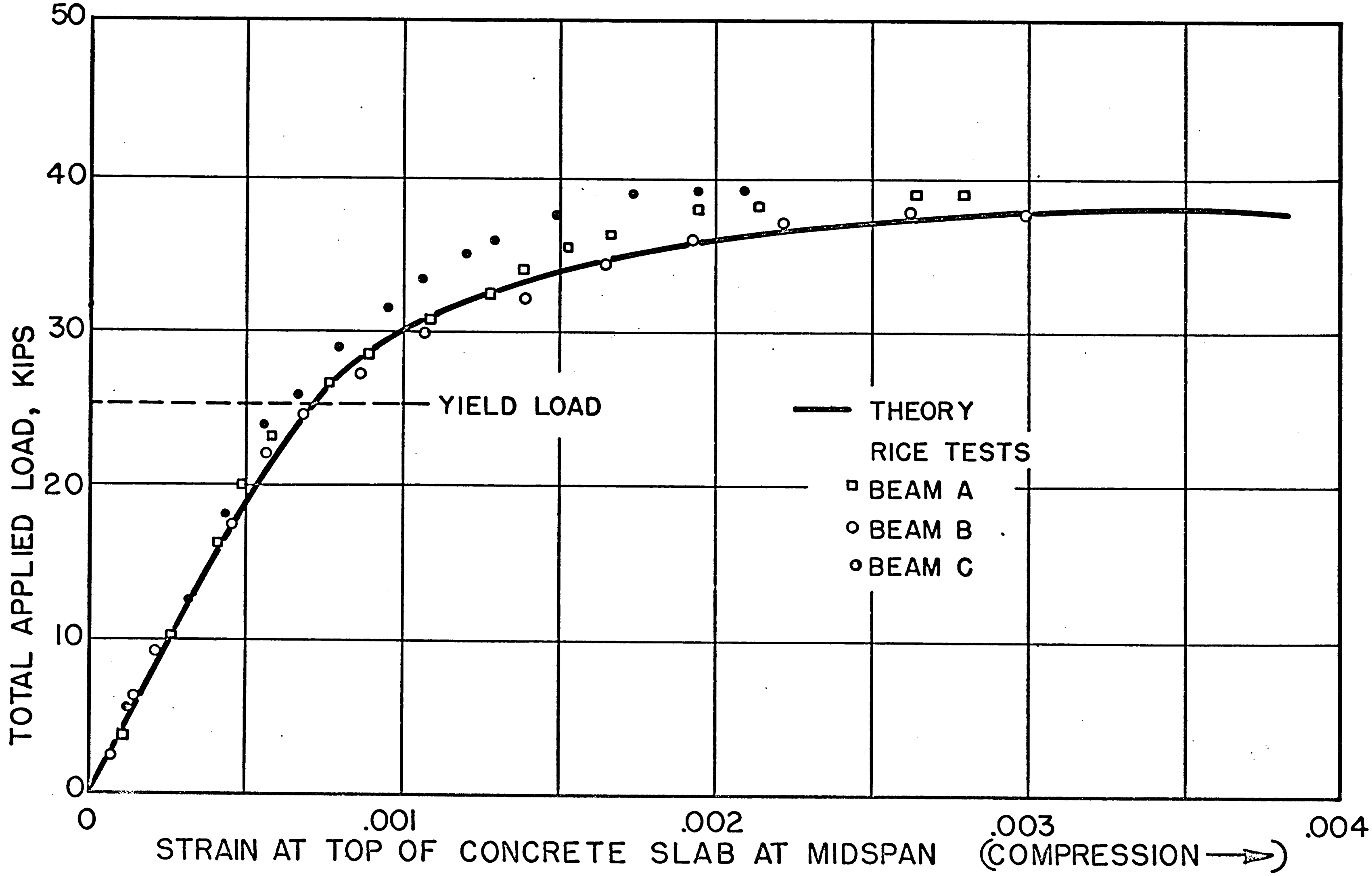

FIG. 23. Analytical and experimental concrete strain results for Rice beams

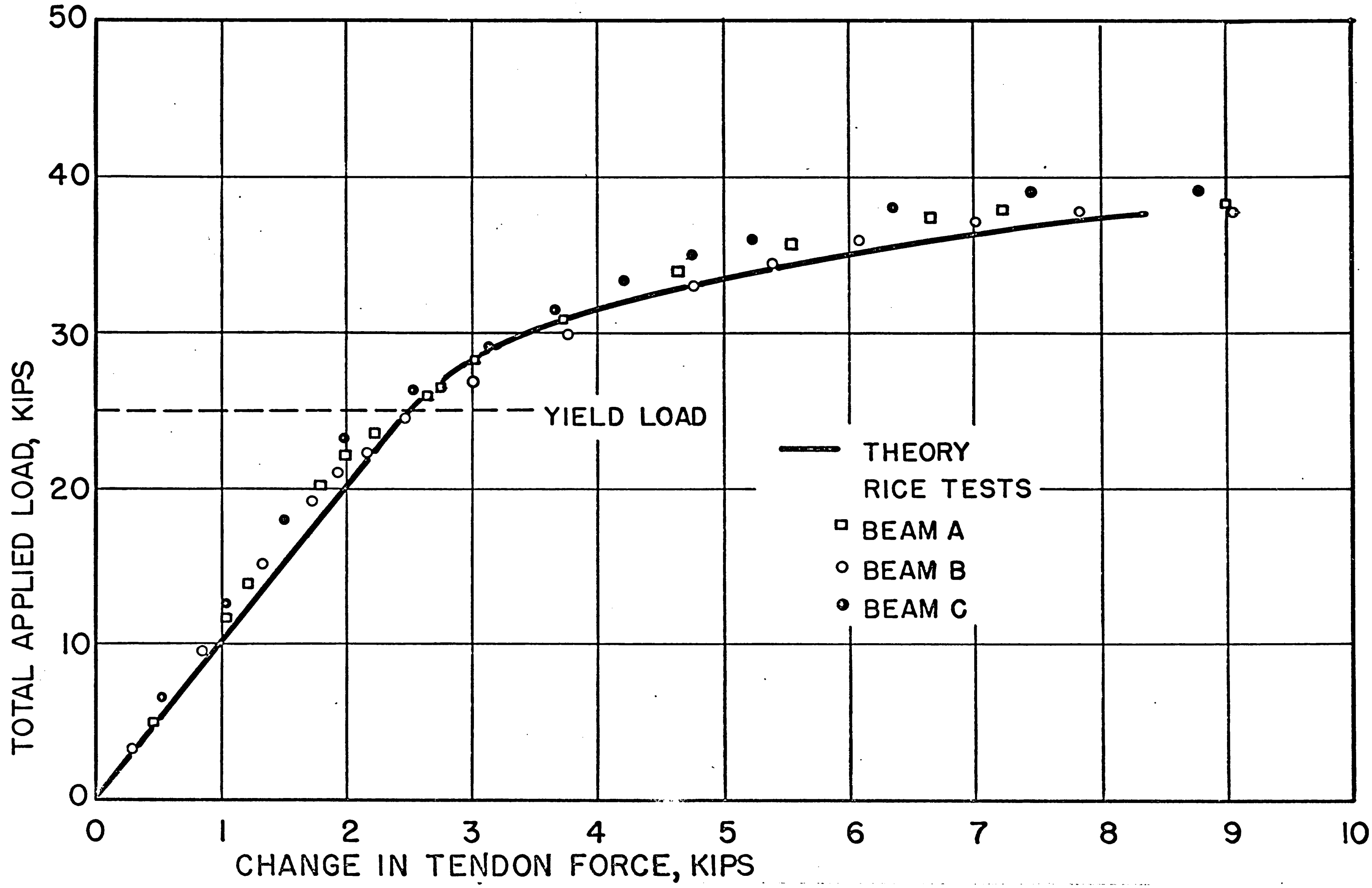

FIG. 24. Analytical and experimental tendon force results for Rice beams

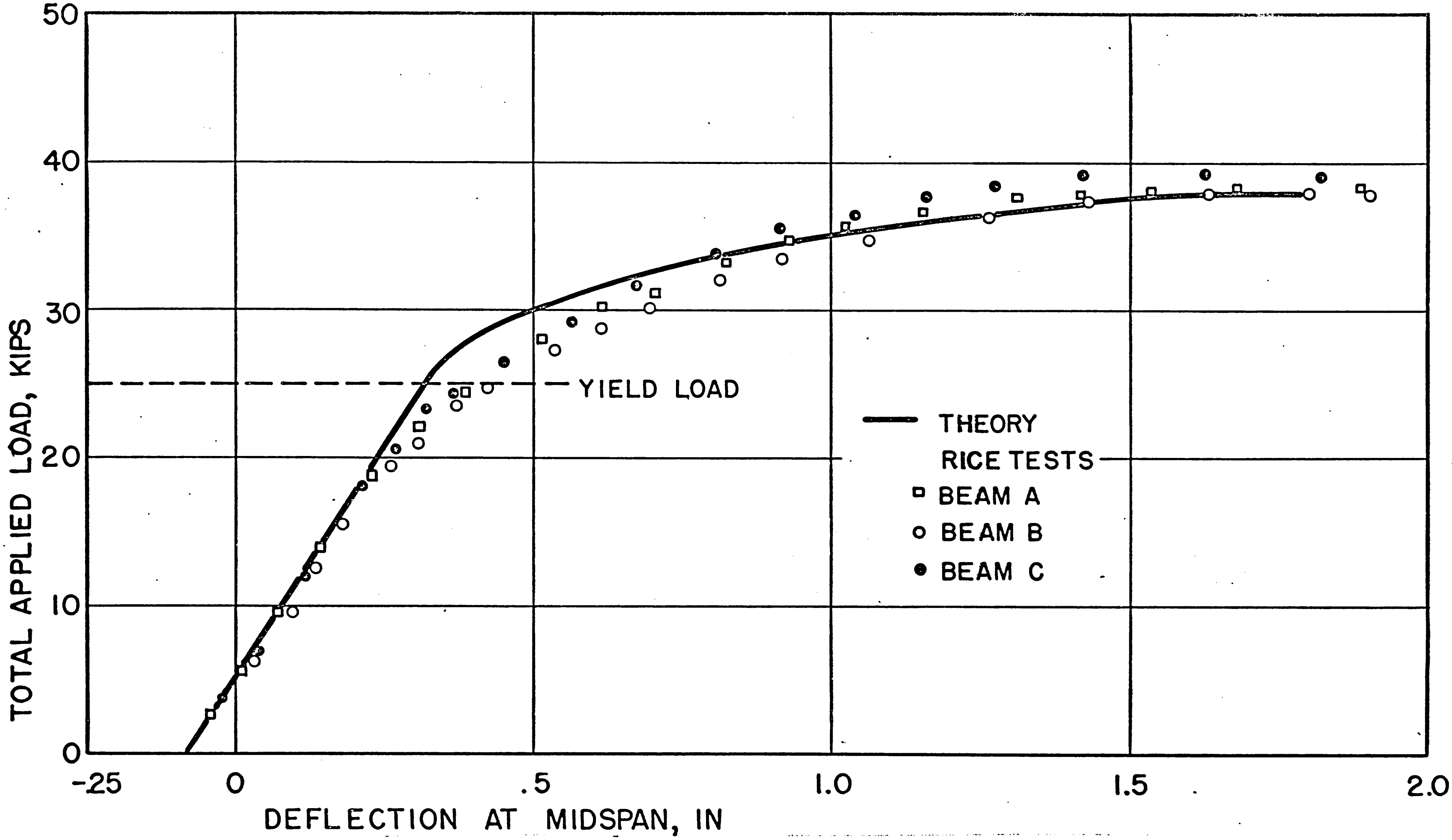

FIG. 25. Analytical and experimental deflection results for Rice beams

4. CONCLUSIONS

Based upon the analytical results obtained and the comparison of the analytical results with available experimental results, the following conclusions are offered:

1. The method of analysis of conventional and prestressed composite beams presented herein gives a reasonable approximation to the behavior of these structures throughout the entire range of loading up to failure.
2. Prestressing a composite beam increases the yield and ultimate loads. Thus a prestressed composite beam is an efficient structure if design is based upon ultimate strength.
3. Prestressing greatly increases the load producing the allowable steel stress, but doesn't significantly increase the load producing the allowable concrete stress. Thus there is some optimum prestress force (about 200 kips for the beams in Fig. 12 and about 75 kips for the beams in Fig. 16) for which the steel and concrete stresses will reach their allowable values at the same value of load. Any prestress force greater than this optimum one will only slightly increase the allowable load of the structure, since the concrete stress governs and is not significantly changed by additional prestress. Thus, if design is based upon allowable stresses, prestressed composite beams will be most efficient only if care is taken to select the proper combination of composite beam and prestress force.
4. Prestressing does not significantly reduce the live load deflection of composite beams. Therefore, if the design of a composite beam is controlled by live load deflection, prestressing may not be appropriate. Prestressing, however, does induce an initial camber which is desirable for certain applications.

5. Large amounts of prestress caused yielding over the support in some of the prestressed composite beams analyzed in this study. This is undesirable and can be prevented by avoiding such large amounts of prestress or by simply shortening the tendon and moving the tendon anchors in from the supports.
6. In none of the structures analyzed did the tendon break, since the tendon is a very ductile element of the structure as compared with the concrete slab. This was true even for beam PH10, the only beam for which the prestress force exceeded the recommended working load for the tendon.
7. The slab thickness is not too important a variable in the behavior of prestressed composite beams. Increasing the slab thickness does increase the ultimate load, but not nearly as much as increasing the prestress force or cover plate size does. The slight increase in the stiffness of the structure afforded by increasing the slab thickness is somewhat offset by the corresponding increase in the dead load of the structure and the initial deflection.

REFERENCES

1. Dischinger, F., "Stahlbrucken im Verbund mit Stahlebeton Druckplatten bei Gleichzeitiger Vorspannung durch Hochwertige Seite", Der Bauingernieur, Vol. 11, 1949.

2. Coff, L., "Composite Floor of Metal and Concrete", U. S. Patent 2,510,958, 1950.

3. Szilard, R., "Design of Prestressed Composite Steel Structures", Journal of the Structural Division, ASCE, Vol. 85, No. ST9, Proc. Paper 2262, November, 1959, pp. 97-124.

4. Hoadley, P. G., "Behavior of Prestressed Composite Steel Beams", Journal of the Structural Division, ASCE, Vol. 89, No. ST3, Proc. Paper 3534, June, 1963, pp. 21-34.

5. "Prestressing Steel Stringers Reduces Bridge Weight by 25%", Engineering News Record, McGraw-Hill Publishing Co., New York, N.Y., Vol. 167, No. 16, October 19, 1961.

6. "Prestressed Steel Girders Carry Prestressed Concrete Floor", Engineering News Record, McGraw-Hill Publishing Co., New York, N.Y., Vol. 172, No. 13, March 26, 1964.

7. "Prestressed Steel Makes a Bridge", Engineering News Record, Vol. 173, No. 19, November 5, 1964.

8. Stras, J. C. III, "An Experimental and Analytical Study of Prestressed Composite Beams", thesis presented to Rice University, Houston, Texas, in 1964, in partial fulfilment of the requirements for the degree of Master of Science.

9. Pfrang, E. O., and Siess, C. P., "Predicting Structural Behavior Analytically", Journal of the Structural Division, ASCE, Vol. 90, No. ST5, Proc. Paper 4110, October, 1964, pp. 99-111.

10. Hognestad, E., "A Study of Combined Bending and Axial Load in Reinforced Concrete Members", Bulletin No. 399, Engrg. Experiment Sta., Univ. of Illinois, Urbana, Ill., 1951.

11. Salvadori, M. G. and Baron, M. L., Numerical Methods in Engineering, Prentice-Hall, Inc., Englewood Cliffs, N. J., 1961, pp. 46-47.

12. "Standard Specifications for Highway Bridges", American Association of State Highway Officials, 1961, Washington, D. C.

13. "Interim Specifications, 1962", AASHO Committee on Bridges and Structures, American Association of State Highway Officials, 1963, Washington, D.C.

14. "Specification for the Design, Fabrication, and Erection of Structural Steel for Buildings", American Institute of Steel Construction, April 17, 1963.

15. "Building Code Requirements for Reinforced Concrete", American Concrete Institute, June, 1963.

16. Viest, I. M., Siess, C. P., Appleton, H. H., and Newmark, N. M., "Full Scale Tests on Channel Shear Connectors and Composite T-Beams", Bulletin No. 405, Engrg. Experiment Sta., Univ. of Illinois, Urbana, Ill., 1952.

17. Culver, C. and Coston, R., "Tests of Composite Beams with Stud Shear Connectors", Journal of the Structural Division, ASCE, Vol. 87, No. ST2, Proc. Paper 2742, February, 1961.

18. Toprac, A. A. "Strength of Three New Types of Composite Beams", American Iron and Steel Institute, Bulletin No. 2, October, 1965.

19. Barnard, P. R., "A Series of Tests on Simply Supported Composite Beams", Journal of the American Concrete Institute, Vol. 61, No. 4, April, 1965, pp. 443-456.

APPENDIX A. EQUATIONS USED IN THE ANALYSIS

1. Coordinate system and sign conventions

The coordinate system used showing the equally spaced node points and the corresponding sign conventions for slope and curvature appear in Fig. A-1. Tensile strains, downward loads, and external moments causing negative curvature were taken as positive.

2. Initial conditions

The strains caused by the prestress force and dead load of the beam were calculated from the following equations.

a. Strains due to prestress

$$\epsilon_{tp} = -\frac{F_p}{E_s}\left(\frac{1}{A_s} - \frac{e_s d_s}{2I_s}\right) \tag{A-1}$$

$$\epsilon_{bp} = -\frac{F_p}{E_s}\left(\frac{1}{A_s} + \frac{e_s d_s}{2I_s}\right) \tag{A-2}$$

where ϵ_{tp} = strain at top of steel beam due to prestress

ϵ_{bp} = strain at bottom of steel beam due to prestress

F_p = prestress force

E_s = modulus of elasticity of steel beam

A_s = area of steel beam cross section

d_s = depth of steel beam

I_s = moment of inertia of steel beam cross section about its centroidal axis

e_s = distance from tendon centroid to centroid of steel beam

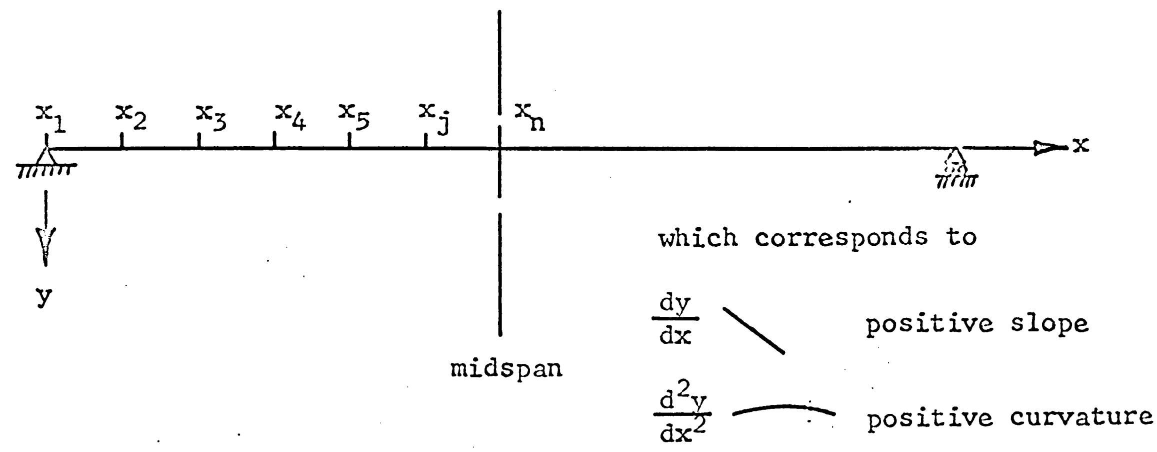

FIG. A-1. Coordinate system used for deflections

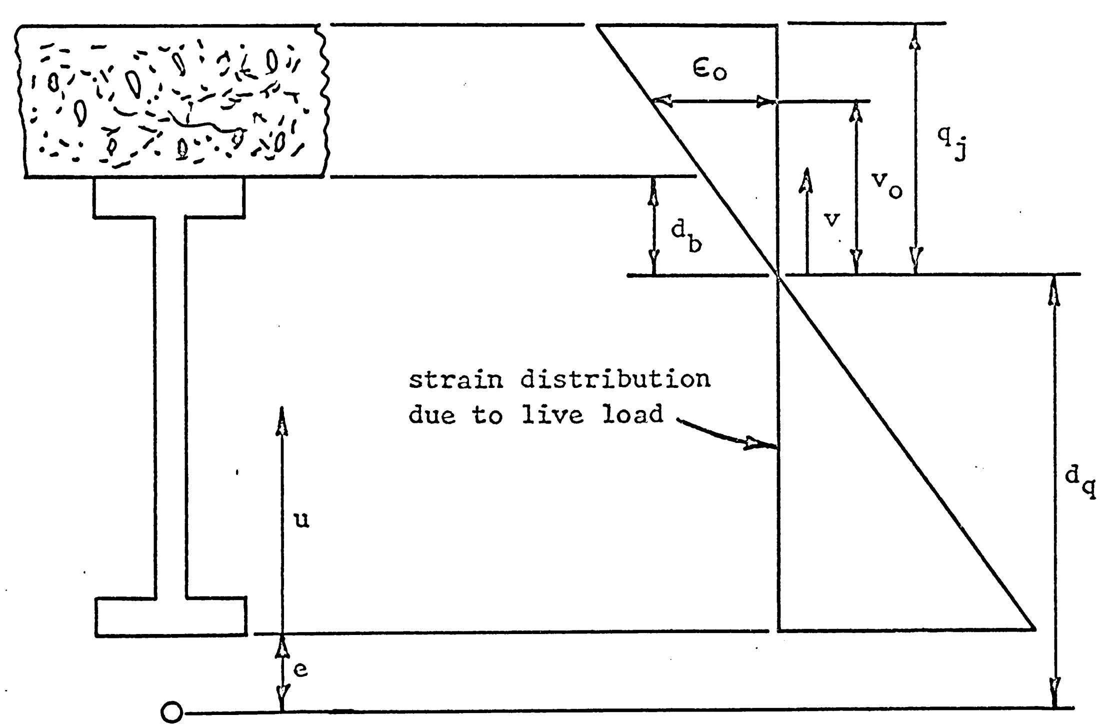

FIG. A-2. Coordinate systems used in integrating stresses

b. Strains due to dead load

$$F_d = \frac{e_s w_d L_s^3}{12 E_s I_s \left(\frac{L_s e_s^2}{E_s I_s} + \frac{L_t}{A_t E_t} + \frac{L_s}{A_s E_s} \right)} \qquad \text{(A-3)}$$

where F_d = increase in tendon force due to dead load

w_d = uniformly distributed dead load of the structure

L_s = span length of the steel beam

L_t = tendon length

E_t = modulus of elasticity of tendon

A_t = area of tendon cross section

$$M_{dj} = \frac{w_d x_j}{2} (L_s - x_j) \qquad \text{(A-4)}$$

where M_{dj} = dead load moment at jth node point

x_j = x coordinate of jth node point

$$\epsilon_{tdj} = -\frac{F_d}{A_s E_s} + \frac{(F_d e_s - M_{dj}) d_s}{2 I_s E_s} \qquad \text{(A-5)}$$

$$\epsilon_{bdj} = -\frac{F_d}{A_s E_s} - \frac{(F_d e_s - M_{dj}) d_s}{2 I_s E_s} \qquad \text{(A-6)}$$

where ϵ_{tdj} = strain at top of steel beam at jth node point due to dead load

ϵ_{bdj} = strain at bottom of steel beam at jth node point due to dead load

c. Total initial strains

$$\epsilon_{tIj} = \epsilon_{tp} + \epsilon_{tdj} \qquad \text{(A-7)}$$

$$\epsilon_{bIj} = \epsilon_{bp} + \epsilon_{bdj} \qquad \text{(A-8)}$$

$$F_{tI} = F_p + F_d \qquad \text{(A-9)}$$

where ϵ_{tIj} = initial strain at top of steel beam at jth node point

ϵ_{bIj} = initial strain at bottom of steel beam at jth node point

F_{tI} = initial tendon force

3. Curvatures

The curvatures at each node point of the beam were found from Eq. A-10.

$$\phi_j = \frac{\epsilon_{tj} - \epsilon_{bj}}{d_s} \qquad \text{(A-10)}$$

where ϕ_j = curvature at jth node point

ϵ_{tj} = strain at top of steel beam at jth node point

ϵ_{bj} = strain at bottom of steel beam at jth node point

4. Slopes and deflections

The slopes and deflections of each node point were found by numerical integration of the curvatures as shown in Eqs. A-11 and A-12.

$$\Theta_j = \int_0^{x_j} \phi(x)dx - \int_0^{x_n} \phi(x)dx \qquad \text{(A-11)}$$

where Θ_j = slope at jth node point

$\phi(x)$ = distribution of curvatures along beam length des-described by values at the discrete node points

n = subscript denoting node point at midspan

$$y_j = \int_0^{x_j} \Theta(x)dx \tag{A-12}$$

where y_j = deflection at jth node point

$\Theta(x)$ = distribution of slope along beam length described by values at the discrete node points

The three-point quadrature formula Eq. A-13 was used for the numerical integration.

$$\int_{x_i}^{x_{i+1}} f(x)dx \cong \frac{h}{12}(5f_i + 8f_{i+1} - f_{i+2}) \tag{A-13}$$

where $f(x)$ = function of x described by discrete values at equally spaced node points

f_i = value of f at ith node point

h = node point spacing

5. Equilibrium equations

The equations of static equilibrium at the jth node point as found by summation of forces and summation of moments about the tendon centroid appear in Eqs. A-14 and A-15. See Fig. 4 for a free body diagram.

$$\sum F_x = \int_A f(y)dA - F_t = 0 \tag{A-14}$$

$$\sum M_t = \int_A f(y)ydA - M_j = 0 \tag{A-15}$$

where $\sum F_x$ = sum of forces in the horizontal direction

F_t = tendon force

$f(y)$ = stress distribution over beam cross section

$\sum M_t$ = sum of moments about tendon centroid

M_j = external moment at x_j

6. Solution of equilibrium equations

For assumed values of F_t and M_j Eqs. 14 and 15 were solved at each node point for ϵ_{bj} and ϵ_{tj}. The integrals in the equations are functions of ϵ_{bj} and ϵ_{tj}. At midspan ϵ_{bj} was known since it was the quantity incremented until failure of the beam, so Eq. 14 was solved for ϵ_{tj} using the method of tangents for a single nonlinear equation, written below in the notation of this thesis.

$$F(\epsilon_{tj},\epsilon_{bj}) - F_t = 0 \tag{A-16}$$

$$\epsilon_{tj} - \epsilon_{tj}\Big|_o = \frac{F(\epsilon_{tj},\epsilon_{bj})}{\left.\dfrac{\partial F(\epsilon_{tj},\epsilon_{bj})}{\partial \epsilon_{tj}}\right|_o} \tag{A-17}$$

where $F(\epsilon_{tj},\epsilon_{bj})$ = internal force at jth node point

o = subscript denoting evalution for current values of the iterates

Then Eq. 14 was solved directly for M_j at midspan.

At the remaining node points Eqs. 14 and 15 were solved simultaneously for the values of ϵ_{tj} and ϵ_{bj}, using the method of tangents for two simultaneous nonlinear equations as shown below.

$$M(\epsilon_{tj},\epsilon_{bj}) - M_j = 0 \tag{A-18}$$

$$\epsilon_{tj} - \epsilon_{tj}\Big|_o = -\frac{F_o \left.\dfrac{\partial M}{\partial \epsilon_{bj}}\right|_o - M_o \left.\dfrac{\partial F}{\partial \epsilon_{bj}}\right|_o}{\left.\dfrac{\partial F}{\partial \epsilon_{tj}}\right|_o \cdot \left.\dfrac{\partial M}{\partial \epsilon_{bj}}\right|_o - \left.\dfrac{\partial M}{\partial \epsilon_{tj}}\right|_o \left.\dfrac{\partial F}{\partial \epsilon_{bj}}\right|_o} \tag{A-19}$$

$$\epsilon_{bj} - \epsilon_{bj}\Big|_o = -\frac{\frac{\partial F}{\partial \epsilon_{tj}}\Big|_o M_o - \frac{\partial M}{\partial \epsilon_{tj}}\Big|_o F_o}{\frac{\partial F}{\partial \epsilon_{tj}}\Big|_o \frac{\partial M}{\partial \epsilon_{bj}}\Big|_o - \frac{\partial M}{\partial \epsilon_{tj}}\Big|_o \frac{\partial F}{\partial \epsilon_{bj}}\Big|_o} \qquad \text{(A-20)}$$

where $M(\epsilon_{tj},\epsilon_{bj})$ = internal moment about tendon centroid at jth node point

The values of the integrals in Eqs. A-14 and A-15 and implicit in Eqs. A-16 and A-18 were found in closed form by breaking the integrals into pieces at each change of width of the cross section and change of stress-strain function. The partial derivatives in Eqs. A-17, A-19, and A-20 were found by differentiation of these integrals using Leibnitz's rule for differentiation of integrals containing a parameter.

The integration over the steel beam cross section involved breaking the cross section up into a number of elastic and plastic elements, and for both elastic and plastic elements, equations for internal force, internal moment, and partial derivatives were obtained.

A coordinate "u" measured upward from the bottom of the steel beam was introduced as shown in Fig. A-2. The strain distribution across the steel beam was given by Eq. A-21.

$$\epsilon_s = \epsilon_{bj} + \phi_j u \qquad \text{(A-21)}$$

The equations for internal force and internal moment for elements of the steel beam were found by substituting Eq. A-21 into the appropriate stress-strain function given in Fig. 2(a) and integrating the resulting function for the stress distribution according to Eqs. A-14 and A-15. The partial derivatives were found by differentiation of the resulting integrals using Leibnitz's rule.

For an elastic element of the steel beam

$$F_e = bE_s\left[\epsilon_{bj}(u_2 - u_1) + \phi_j \frac{u_2^2 - u_1^2}{2}\right] \tag{A-22}$$

$$\frac{\partial F_e}{\partial \epsilon_{tj}} = bE_s \frac{u_2^2 - u_1^2}{2d_s} \tag{A-23}$$

$$\frac{\partial F_e}{\partial \epsilon_{bj}} = bE_s \left[(u_1 - u_2) - \frac{u_2^2 - u_1^2}{2d_s}\right] \tag{A-24}$$

$$M_e = bE_s\left[\epsilon_{bj} \frac{u_2^2 - u_1^2}{2} + \phi_j \frac{u_2^3 - u_1^3}{3}\right] + F_e e \tag{A-25}$$

$$\frac{\partial M_e}{\partial \epsilon_{tj}} = bE_s \frac{u_2^3 - u_1^3}{3d_s} + e\frac{\partial F_e}{\partial \epsilon_{tj}} \tag{A-26}$$

$$\frac{\partial M_e}{\partial \epsilon_{bj}} = bE_s\left(\frac{u_2^2 - u_1^2}{2} - \frac{u_2^3 - u_1^3}{3d_s}\right) + e\frac{\partial F_e}{\partial \epsilon_{bj}} \tag{A-27}$$

where F_e = resultant internal force over elastic element of steel beam

u_1 = lower u coordinate of elastic element

u_2 = upper u coordinate of elastic element

M_e = resultant internal moment over elastic element of steel beam

e = distance from bottom of steel beam to tendon centroid

b = width of element of steel beam

For a plastic element of the steel beam

$$F_y = \pm bf_y(u_4 - u_3) \tag{A-28}$$

$$M_y = \pm bf_y \frac{u_4^2 - u_3^2}{2} + F_y e \tag{A-29}$$

$$\frac{\partial F_y}{\partial \epsilon_{tj}} = \frac{\partial F_y}{\partial \epsilon_{bj}} = \frac{\partial M_y}{\partial \epsilon_{tj}} = \frac{\partial M_y}{\partial \epsilon_{bj}} = 0 \tag{A-30}$$

where F_y = resultant internal force over plastic element of steel beam

u_4 = upper u coordinate of plastic element

u_3 = lower u coordinate of plastic element

M_y = resultant internal moment over plastic element

The strain distribution in the concrete slab was specified by the quantities calculated in Eqs. A-31, A-32, A-33, and A-34.

$$\epsilon_{tPj} = \epsilon_{tj} - \epsilon_{tIj} \tag{A-31}$$

$$\epsilon_{bPj} = \epsilon_{bj} - \epsilon_{bIj} \tag{A-32}$$

$$\phi_{Pj} = \frac{\epsilon_{tPj} - \epsilon_{bPj}}{d_s} \tag{A-33}$$

$$q_j = d_c + \frac{\epsilon_{tPj}}{\phi_{Pj}} \tag{A-34}$$

where ϵ_{tPj} = strain at top of steel beam due to live load at jth node point

ϵ_{bPj} = strain at bottom of steel beam due to live load at jth node point

ϕ_{Pj} = curvature at jth node point due to live load

q_j = distance from point of zero strain due to live load to the top of the concrete slab

The integration of stresses over the concrete slab cross section was done in a slightly different manner than for the steel beam. There were five possible distributions of stress in the concrete slab labeled as cases 1 to 5 in Fig. A-3. A coordinate "v" as shown in Fig. A-2 was introduced measured upward from the point of zero strain due to live load. General expressions were obtained for the internal force and the internal moment across the concrete slab cross section. The partial derivatives were obtained by differentiating these expressions using Leibnitz's rule.

The strain distribution in the concrete was found from Eq. A-35.

$$\epsilon_c = \phi_{Pj} v \tag{A-35}$$

The "v" coordinate v_o of the point where the concrete strain equals ϵ_o, the value of strain at which the change in stress-strain function occurs, see Fig. A-2, was found from Eq. A-36.

$$v_o = \frac{\epsilon_o}{\phi_{Pj}} \tag{A-36}$$

Upon substitution of Eq. A-35 into the stress-strain relation given in Fig. 2(b) for the concrete slab, integration of the stress function obtained and differentiation of the result, the following expressions were obtained.

$$F_c = f''_c b_c \left\{ \frac{\phi_{Pj}}{\epsilon_o} \left[(v_2^2 - v_1^2) - \frac{\phi_{Pj}}{3\epsilon_o} (v_2^3 - v_1^3) \right] + \right.$$

$$\left. (1 + \frac{.15\epsilon_o}{\epsilon_u - \epsilon_o})(v_4 - v_3) - \frac{.075\phi_{Pj}}{\epsilon_u - \epsilon_o}(v_4^2 - v_3^2) \right\} \tag{A-37}$$

$$\frac{\partial F_c}{\partial \epsilon_{tj}} = f_c''b_c\left\{\frac{1}{\epsilon_o d_s}\left[(v_2^2 - v_1^2) - \frac{2\phi_{Pj}}{3\epsilon_o}(v_2^3 - v_1^3)\right] + \right.$$

$$\delta_1(v_2)\frac{\partial v_2}{\partial \epsilon_{tj}} - \delta_1(v_1)\frac{\partial v_1}{\partial \epsilon_{tj}} - \frac{.075(v_4^2 - v_3^2)}{d_s(\epsilon_u - \epsilon_o)} +$$

$$\left.\delta_2(v_4)\frac{\partial v_4}{\partial \epsilon_{tj}} - \delta_2(v_3)\frac{\partial v_3}{\partial \epsilon_{tj}}\right\} \qquad \text{(A-38)}$$

$$\frac{\partial F_c}{\partial \epsilon_{bj}} = f_c''b_c\left\{\frac{1}{\epsilon_o d_s}\left[-(v_2^2 - v_1^2) + \frac{2\phi_{Pj}(v_2^3 - v_1^3)}{3\epsilon_o}\right] + \right.$$

$$\delta_1(v_2)\frac{\partial v_2}{\partial \epsilon_{bj}} - \delta_1(v_1)\frac{\partial v_1}{\partial \epsilon_{bj}} + \frac{.075(v_4^2 - v_3^2)}{d_s(\epsilon_u - \epsilon_o)} +$$

$$\left.\delta_2(v_4)\frac{\partial v_4}{\partial \epsilon_{bj}} - \delta_2(v_3)\frac{\partial v_3}{\partial \epsilon_{bj}}\right\} \qquad \text{(A-39)}$$

$$M_c = f_c''b_c\left\{\frac{\phi_{Pj}}{\epsilon_o}\left[\frac{2(v_2^3 - v_1^3)}{3} - \frac{\phi_{Pj}(v_2^4 - v_1^4)}{4\epsilon_o}\right] + \right.$$

$$\left.\left[1 + \frac{.15\epsilon_o}{(\epsilon_u - \epsilon_o)}\right]\frac{(v_4^2 - v_3^2)}{2} - \frac{.05\phi_{Pj}(v_4^3 - v_3^3)}{(\epsilon_u - \epsilon_o)}\right\} + F_c d_q \qquad \text{(A-40)}$$

$$\frac{\partial M_c}{\partial \epsilon_{tj}} = f_c''b_c\left\{\frac{1}{\epsilon_o d_s}\left[\frac{2}{3}(v_2^3 - v_1^3) - \frac{\phi_{Pj}(v_2^4 - v_1^4)}{2\epsilon_o}\right] + \right.$$

$$\delta_3(v_2)\frac{\partial v_2}{\partial \epsilon_{tj}} - \delta_3(v_1)\frac{\partial v_1}{\partial \epsilon_{tj}} - \frac{.05(v_4^3 - v_3^3)}{d_s(\epsilon_u - \epsilon_o)}$$

$$\left. + \delta_4(v_4)\frac{\partial v_4}{\partial \epsilon_{tj}} - \delta_4(v_3)\frac{\partial v_3}{\partial \epsilon_{tj}}\right\} - F_c\frac{\partial q_j}{\partial \epsilon_{tj}} + \frac{\partial F_c}{\partial \epsilon_{tj}}d_q \tag{A-41}$$

$$\frac{\partial M_c}{\partial \epsilon_{bj}} = f_c''b_c\left\{\frac{1}{\epsilon_o d_s}\left[-\frac{2}{3}(v_2^3 - v_1^3) + \frac{\phi_{Pj}(v_2^4 - v_1^4)}{2\epsilon_o}\right] + \right.$$

$$\delta_3(v_2)\frac{\partial v_2}{\partial \epsilon_{bj}} - \delta_3(v_1)\frac{\partial v_1}{\partial \epsilon_{bj}} + \frac{.05(v_4^3 - v_3^3)}{d_s(\epsilon_u - \epsilon_o)} + \delta_4(v_4)\frac{\partial v_4}{\partial \epsilon_{bj}}$$

$$\left. - \delta_4(v_3)\frac{\partial v_3}{\partial \epsilon_{bj}}\right\} - F_c\frac{\partial q_j}{\partial \epsilon_{bj}} + \frac{\partial F_c}{\partial \epsilon_{bj}}d_q \tag{A-42}$$

where

$$\delta_1(v) = \frac{\phi_{Pj}}{\epsilon_o}\left(2v - \frac{v^2\phi_{Pj}}{\epsilon_o}\right) \tag{A-43}$$

$$\delta_2(v) = 1 + \frac{.15\epsilon_o}{\epsilon_u - \epsilon_o} - \frac{.15\phi_{Pj}\, v}{\epsilon_u - \epsilon_o} \tag{A-44}$$

$$\delta_3(v) = v\delta_1(v) \tag{A-45}$$

$$\delta_4(v) = v\delta_2(v) \tag{A-46}$$

$$d_q = d_s + d_c + e - q_j \tag{A-47}$$

and where F_c = resultant internal force over concrete slab cross section

M_c = resultant internal moment about tendon centroid over concrete slab cross section

d_q = distance from tendon centroid to point of zero strain due to live load

b_c = width of concrete slab

d_b = distance from point of zero strain due to live load to the bottom of the concrete slab

These equations were applied by substituting the appropriate limits which are given in Table A-1 for each of the five possible distributions of stress. Other quantities needed in these equations were calculated from the expressions appearing below.

$$\frac{\partial v_o}{\partial \epsilon_{tj}} = -\frac{\epsilon_o / d_s}{\phi^2_{Pj}} \tag{A-48}$$

$$\frac{\partial v_o}{\partial \epsilon_{bj}} = \frac{\epsilon_o / d_s}{\phi^2_{Pj}} \tag{A-49}$$

$$\frac{\partial q_j}{\partial \epsilon_{tj}} = \frac{\epsilon_{tPj} / d_s}{\phi^2_{Pj}} \tag{A-50}$$

$$\frac{\partial q_j}{\partial \epsilon_{bj}} = \frac{\phi_{Pj} - \epsilon_{tPj} / d_s}{\phi^2_{Pj}} \tag{A-51}$$

$$\frac{\partial d_b}{\partial \epsilon_{tj}} = \frac{\partial q_j}{\partial \epsilon_{tj}} \tag{A-52}$$

$$\frac{\partial d_b}{\partial \epsilon_{bj}} = \frac{\partial q_j}{\partial \epsilon_{bj}} \tag{A-53}$$

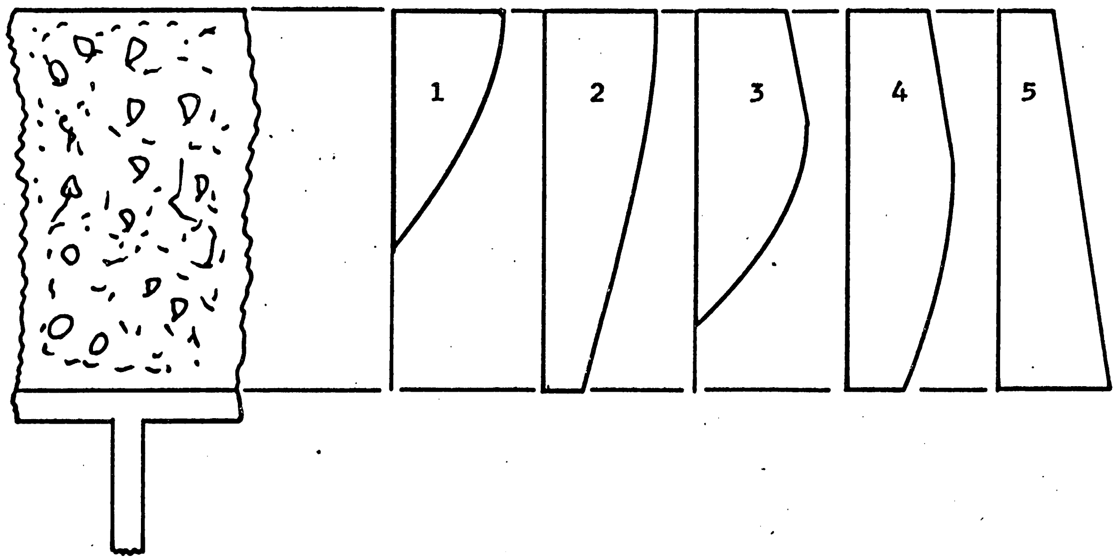

FIG. A-3. Possible stress distributions in concrete slab

case	v_1	v_2	v_3	v_4
1	0	q_j	0	0
2	d_b	q_j	0	0
3	0	v_0	v_0	q_j
4	d_b	v_0	v_0	q_j
5	0	0	d_b	q_j

TABLE A-1. Limits of integration for each possible concrete stress distribution

The total values of $F(\epsilon_{tj},\epsilon_{bj})$, $M(\epsilon_{tj},\epsilon_{bj})$, and the partial derivatives were found by summing the results for each element of the steel beam and for the concrete slab.

7. Determination of the tendon deformation from the beam deformations

The tendon strain is the same as the average strain in a fictitious beam "fiber" at the location of the tendon centroid. This average strain was found by integrating numerically the strains of this "fiber" along the length of the beam using Eq. A-13 and dividing the result by the tendon length. The equations for these calculations appear below.

$$\epsilon_{fj} = \epsilon_{bj} - e\phi_j \tag{A-54}$$

$$\epsilon_{ta} = \frac{2\int_{x_1}^{x_n} \epsilon_f(x)dx}{L_t} \tag{A-55}$$

where ϵ_{fj} = strain in fictitious "fiber" at jth node point

ϵ_{ta} = tendon strain

$\epsilon_f(x)$ = distribution of strain in fictitious "fiber" along the beam length specified by the values at the node points

APPENDIX B. NOTATION

The symbols used in this thesis are defined where they first occur, and are listed below:

A_s	Area of steel beam cross section
A_t	Area of tendon cross section
b	Width of steel beam element
b_c	Width of concrete slab
d_b	Distance from point of zero strain due to live load to the bottom of the concrete slab
d_c	Depth of the concrete slab
d_q	Distance from tendon centroid to point of zero strain due to live load
d_s	Depth of steel beam
e	Distance from bottom of steel beam to tendon centroid
e_s	Distance from tendon centroid to centroid of steel beam
E_c	Initial tangent modulus of elasticity of the concrete
E_s	Modulus of elasticity of the steel beam
E_t	Modulus of elasticity of the tendon
f_c	Concrete stress
f'_c	Compressive strength of the concrete determined from cylinder tests
f''_c	Compressive strength of concrete in beams
f_i	Value of f(x) at ith node point
f_s	Stress in steel beam
f_y	Yield stress of steel beam
$f(x)$	Function of x described by discrete values at equally spaced node points

$f(y)$	Stress distribution over beam cross section
F_c	Resultant internal force over concrete slab cross section
F_d	Increase in tendon force due to dead load
F_e	Resultant internal force over an elastic element of the steel beam
F_I	Initial tendon force
F_t	Tendon force
F_p	Prestress force
F_y	Resultant internal force over plastic element of steel beam
$F(\epsilon_b,\epsilon_t)$	Resultant internal force over beam cross section
h	Node point spacing
I_s	Moment of inertia of steel beam cross section about its centroidal axis
L_s	Span length
L_t	Tendon length
M_c	Resultant internal moment about tendon centroid over concrete slab cross section
M_{dj}	Dead load moment at jth node point
M_e	Resultant internal moment about tendon centroid over an elastic element of the steel beam
M_j	External moment at x_j
M_x	External moment
M_y	Resultant internal moment about tendon centroid over plastic element of the steel beam
$M(\epsilon_b,\epsilon_t)$	Resultant internal moment about tendon centroid at beam cross section

P	Concentrated live load
q_j	Distance from top of concrete slab to point of zero strain due to live load
u	Coordinate measured upward from the bottom of the steel beam
u_1	Lower u coordinate of an elastic element of the steel beam
u_2	Upper u coordinate of an elastic element of the steel beam
u_3	Lower u coordinate of a plastic element of the steel beam
u_4	Upper u coordinate of a plastic element of the steel beam
w	Uniformly distributed live load
w_d	Uniformly distributed dead load
x	Coordinate measured from beam support along the beam axis
y	Vertical deflection of the beam
v	Coordinate measured upward from the point of zero strain due to live load
v_o	v coordinate where $\epsilon_c = \epsilon_o$
v_1-v_4	Limits of integration specified in Table A-1
$\delta_1(v)$-$\delta_4(v)$	Integrands used in Leibnitz's rule
ϵ_b	Strain at bottom of steel beam
ϵ_{bd}	Strain at bottom of steel beam due to dead load
ϵ_{bI}	Initial strain at bottom of steel beam
ϵ_{bp}	Strain at bottom of steel beam due to prestress
ϵ_{bP}	Strain at bottom of steel beam due to live load
ϵ_c	Concrete strain
ϵ_f	Strain in fictious beam fiber at level of tendon centroid
ϵ_o	Compressive strain in concrete corresponding to maximum stress

ϵ_s	Strain in steel beam
ϵ_t	Strain at top of steel beam
ϵ_{ta}	Tendon strain
ϵ_{tI}	Initial strain at top of steel beam
ϵ_{td}	Strain at top of steel beam due to dead load
ϵ_{tp}	Strain at top of steel beam due to prestress
ϵ_{tP}	Strain at top of steel beam due to live load
ϵ_u	Maximum strain in concrete at crushing
ϵ_y	Yield strain of steel beam
θ	Slope of beam
ΣF_x	Sum of forces in the horizontal direction
ΣM_t	Sum of moments about the tendon centroid
ϕ	Curvature
ϕ_P	Curvature due to live load

Subscript "j" denotes value of quantity at a particular node point

Subscript "n" denotes the node point at midspan

Subscript "o" denotes evaluation for the current values of the iterates in the method of tangents

APPENDIX C. LISTINGS OF COMPUTER PROGRAMS

Listings of the Fortran computer programs and subroutines used to analyze the prestressed and conventional composite beams studied appear on the following pages.

The main program PSCOM for analyzing prestressed composite beams, uses subroutines FMP, PLOAD, EBMI, CSD, INTEG, PINT, SLOPE, STE, and STP. The main program COMP for analyzing conventional composite beams uses all these subroutines except PINT.

FMP is a subroutine which calculates from a given strain distribution the internal force, internal moment, and partial derivatives of the internal force and internal moment with respect to the strains. PLOAD and EBMI are subroutines which calculate the live load moment from the external moment and the external moment from the live load, respectively. Listings for PLOAD and EBMI are given for each of the live loads considered in this study. Subroutine CSD calculates the slopes and deflections along the beam length by numerical integration of the curvatures. INTEG a numerical integration subroutine which finds the integral at each node point of any function specified by values at the node points. PINT is a parabolic interpolation subroutine used to interpolate between the points given for the tendon stress-strain relation. SLOPE is a subroutine which corrects the values of the integral of the curvature to values of slope by making them satisfy the condition that the slope at midspan equal zero. Subroutines STE and STP calculate the internal force, internal moment, and partial derivatives for elastic and plastic elements of the steel beam cross section, respectively.

```
$IBFTC PSCOM
C*****PSCOM-PROGRAM FOR ANALYSIS OF PRESTRESSED COMPOSITE BEAMS
  101 FORMAT(28H PRESTRESS HAS YIELDED BEAM.)
  102 FORMAT(1X,7E10.2)
  104 FORMAT(1X,7F10.5)
  105 FORMAT(1X,6E15.7)
  106 FORMAT(1X,2I5)
  107 FORMAT(20X,2E15.7)
  108 FORMAT(1X,I7,2E15.8)
  110 FORMAT(72H1RESULTS FROM THE ANALYSIS BY THE RICE UNIVERSITY IBM 70
     140 COMPUTER OF A)
  111 FORMAT(44H SIMPLY-SUPPORTED PRESTRESSED COMPOSITE BEAM)
  112 FORMAT(17H0 BEAM PROPERTIES/12H01.MATERIALS/15H0  A.STEEL BEAM)
  113 FORMAT(17H    YIELD STRESS=E15.8,18HPSI  YIELD STRAIN=E15.8,6H IN/
     1IN/26H    MODULUS OF ELASTICITY=E15.8,4H PSI)
  137 FORMAT(18H0  B.CONCRETE SLAB)
  114 FORMAT(22H    ULTIMATE STRENGTH=E15.8,4H PSI/32H    STRAIN AT ULTI
     1MATE STRENGTH=E15.8,6H IN/IN)
  138 FORMAT(20H    LIMITING STRAIN=E15.8,6H IN/IN)
  127 FORMAT(20H    TANGENT MODULUS=E15.8)
  115 FORMAT(11H0  C.TENDON/15H    STRESS, PSI,11X,13HSTRAIN, IN/IN)
  116 FORMAT(3X,E15.8,7X,E15.8)
  117 FORMAT(26H    MODULUS OF ELASTICITY=E15.8,4H PSI/28H0 2.CROSS SECT
     1ION DIMENSIONS/15H0  A.STEEL BEAM/11H    WEIGHT=E15.8,6H LB/FT)
  118 FORMAT(9H    AREA=E15.8,4H IN2,15X,6HDEPTH=E15.8,3H IN/34H    RECT
     1ANGLES, FROM BOTTOM TO TOP/8H0 NUMBER, 9X,5HDEPTH,10X,5HWIDTH)
  119 FORMAT(                                    22H    MOMENT OF INERTIA=E
     115.8,4H IN4/18H0  B.CONCRETE SLAB)
  120 FORMAT(11H    WEIGHT=E15.8,7H LB/FT3,13X,6HDEPTH=E15.8,3H IN/11H
     1  WIDTH =E15.8,3H IN/11H0  C.TENDON)
  121 FORMAT(9H    AREA=E15.8,4H IN2,14X,7HWEIGHT=E15.8,6H LB/FT/ 51H
     1 DISTANCE FROM BEAM BOTTOM FLANGE TO TENDON C/L=E15.8,3H IN)
  122 FORMAT(21H0 3.LINEAR DIMENSIONS/8H    SPAN=E15.8,3H IN13X,14HTENDON
     1 LENGTH=E15.8,3H IN/29H   DISTANCE FROM C/L TO LOAD=E15.8,3H IN)
  140 FORMAT(19H0 4. TOTAL WEIGHT =E15.8,3H LB)
  123 FORMAT(20H0 5.PRESTRESS FORCE=E15.8,3H LB/39H0 6.DEAD LOADS FROM A
```

```
   1DJOINING STRUCTURE/17H   ON STEEL BEAM=E15.8,6H LB/FT/21H   ON COM
   2POSITE BEAM=E15.8,6H LB/FT/21H0 7.STRAIN INCREMENT=E15.8,6H IN/IN/
   315H0 8.NODE POINTS)
124 FORMAT(21H    NODE POINT NUMBER,21X,16HX COORDINATE, IN)
125 FORMAT(11X,I5,25X,E15.8)
126 FORMAT(28H0TOLERANCE  USED BY PROGRAM=E15.8)
128 FORMAT(29H0 BEHAVIOR UNDER APPLIED LOAD)
129 FORMAT(8H0  LOAD=E15.8)
130 FORMAT(7H0 NODE ,13HSTRAIN AT TOP,3X,13HSTRAIN AT TOP,3X,9HSTRAIN
   1AT,7X,11HDISTANCE TO)
131 FORMAT(7X,11HOF CONCRETE,5X,14HOF STEEL BEAM,,2X,15HBOTTOM OF STEE
   1L,1X,13HPOINT OF ZERO)
132 FORMAT(7X,11HSLAB, IN/IN,5X,5HIN/IN,11X,11HBEAM, IN/IN,5X,10HSTRAI
   1N, IN)
133 FORMAT(I6,1X,E15.8,1X,E15.8,1X,E15.8,1X,E15.8)
134 FORMAT(7H0 NODE ,9HCHANGE IN,7X,16HCURVATURE, IN-1 ,14HSLOPE, IN/I
   1N  ,2X,13HDEFLECTION,IN)
135 FORMAT(7X,15HCURVATURE, IN-1)
136 FORMAT(14H  CABLE FORCE=E15.8,3H LB,5X,7HCHANGE=E15.8,3H LB/16H  T
   1ENDON STRAIN=E15.8)
    DIMENSION DEC (10),D0(10) ,WF(10),PL(200),CEL(10),S(10),D1(10)
    DIMENSION ARE(8),DEP(8)
    COMMON BEY,BFY,BE,EO,C1,EE,DH,EC,BA,BD,CD,                    EBM,
   1TOLE,FOC,BM,DFDET,DFDEB,DMDET,DMDEB,      WID(8),DST(8),SE(8),L,I,
   2ET(10,200) ,EB(10,200) ,D2(10),D(10),D2I(10),Q(10),ECI(10),IF(200)
    READ(5,106)NP
    DO33NA=1,NP
    READ(5,104)CD,CB,CW
    READ(5,106)NR
    READ(5,104)(DEP(J),WID(J),J=1,NR)
    DST(1)=0.
    DST(2)=0.
    BA=0.
    SM=0.
    DO9J=1,NR
    ARE(J)=DEP(J)*WID(J)
```

```
      DST(J+1)=DST(J)+DEP(J)
      BA=BA+ARE(J)
    9 SM=SM+ARE(J)*(DST(J)+DEP(J)*.5)
      BW=3.4*BA
      YB =SM/BA
      BI=0.
      DO8J=1,NR
    8 BI=BI+WID(J)*DEP(J)**3/12.+ARE(J)*(YB -(DST(J)+DEP(J)*.5))**2
      BD=DST(NR+1)
      BST=BI/(BD-YB )
      BSB=BI/YB
      READ(5,104)BL,WL,WA,WW,EC,DL,DPL,TOLE,TOLF
      READ(5,102)FC,    EU,BFY,BEY,WE,P,HW
      READ(5,106)NO,NW
      READ(5,102)(WF(J),J=1,NW)
      SULT=NW
      SULT=SULT*HW
      BE=BFY/BEY
      WRITE(6,110)
      WRITE(6,111)
      WRITE(6,112)
      WRITE(6,113)BFY,BEY,BE
      WRITE(6,137)
      F2C=.85*FC
      CT=1.8E6-460.*F2C
      EO=2.*F2C/CT.
      WRITE(6,114)FC,EO
      WRITE(6,138)EU
      WRITE(6,127)CT
      WRITE(6,115)
      DO 17 J=1,NW
      Z=J-1
      Z=Z*HW
   17 WRITE(6,116)WF(J),Z
      WRITE(6,117)WE,BW
      WRITE(6,118)BA,BD
```

```
      WRITE(6,108)(J,DEP(J),WID(J),J=1,NR)
      WRITE(6,119)    BI
      WRITE(6,120)CW,CD,CB
      WRITE(6,121)WA,WW,EC
      WRITE(6,122)BL,WL,DL
      TET= P*(EC+YB    )    /(BST   *BE)-P/(BA*BE)
      TEB=-P*(EC+YB    )    /(BSB   *BE)-P/(BA*BE)
      WRITE(6,105)TEB,TET
      IF(BEY+TEB)1,1,2
    1 WRITE(6,101)
      GO TO 33
    2 CONTINUE
      Z=NO-1
      SI=BL/(2.*Z)
      W=(BW+WW+CB*CD*CW/144.)/12.
      TW=W   *BL
      READ(5,104)DLS,DLC
      WRITE(6,140)TW
      WRITE(6,123)P,DLS,DLC,DPL
      WRITE(6,124)
      DLC=DLC/12.
      W=W+DLS/12.
      FD=(YB   +EC)*BL**3*W/(BE*BI*12.*(BL*(YB   +EC)**2/(BE*BI)+
     1WL/(WA*WE)+BL/(BA*BE)))
      TEB=TEB-FD/(BA*BE)-FD*(EC+YB    )    /(BSB*BE)
      TET=TET-FD/(BA*BE)+FD*(EC+YB    )    /(BST*BE)
      DO3I=1,NO
      Z=I-1
      S(I)=Z*SI
      WRITE(6,125)I,S(I)
      EB(I,1)=TEB+W*S(I)*(BL-S(I))*BD/(4.*BE*BI)
      ET(I,1)=TET-W*S(I)*(BL-S(I))*BD/(4.*BE*BI)
      D(I)=0.
      ECT(I)=0.
      Q(I)=0.
      D2I(I)=(ET(I,1)-EB(I,1))/BD
```

```
    3 D2(I)=D2I(I)
      WRITE(6,126)TOLE
      STEN=(P+FD)/(WE*WA)
      DCF=0.
      TF(1)=FD+P
      PL(1)=0.
      EE=EU-EO
      DH=1.+.15*EO/EE
      L=1
      TCA=CD*CB*CT/BE
      TA=TCA+BA
      TQ=(TCA*CD*.5+BA*(CD+BD-YB))/(TA)
      TI=BI+TCA*CD*CD/12.+TCA*(TQ-CD*.5)**2   +BA*(CD+BD-YB-TQ)**2
      ETS=CD+BD+EC-TQ
      EB(NO,2)=DPL+EB(NO,1)
      EBM=(EB(NO,2)-EB(NO,1))*(TI*BE)/(CD+BD-TQ)
      BL2=BL*.5
      TF(2)=TF(1)
      ET(NO,2)=ET(NO,1)+EBM*(CD-TQ)/(TI*BE)
      CALL SSWTCH(2,J2)
      IF(J2.EQ.1)WRITE(6,105)TQ,TI,EB(NO,2),EBM,       ET(NO,2)
      C1=F2C*CB
      WRITE(6,128)
   37 WRITE(6,129)PL(L)
      WRITE(6,136)TF(L),DCF,STEN
      CALL CSD(SI,NO,D2,D1,D0)
      WRITE(6,130)
      WRITE(6,131)
      WRITE(6,132)
      WRITE(6,133)(J,ECT(J),ET(J,L),EB(J,L), Q(J),J=1,NO)
      WRITE(6,134)
      WRITE(6,135)
      WRITE(6,133)(J, D(J),D2(J),D1(J),D0(J),J=1,NO)
      DO72J=1,NO
      IF(EU-ECT(J))72,72,33
   72 CONTINUE
```

```
      IF(STEN-SULT)10,10,33
   10 L=L+1
      KF=1
      I=NO
      EB(NO,L)=EB(NO,L-1)+DPL
      CALL SSWTCH(3,J3)
      IF(J3.EQ.1)WRITE(6,105)EB(I,L)
      IF(L.GT.3)GO TO 4
      GO TO 5
    4 TF(L)= TF(L-3)+3.*(TF(L-1)-TF(L-2))
      ET(NO,L)= ET(NO,L-3)+3.*(ET(NO,L-1)-ET(NO,L-2))
      GO TO 36
    5 IF(L-2)15,36,15
   15 TF(L)=TF(L-1)*2.-TF(L-2)
      ET(NO,L)=2.*ET(NO,L-1)-ET(NO,L-2)
   36 EBM=0.
      CALL FMP(NR)
      COR=FOC/DFDET
      IF(J3.EQ.1)WRITE(6,105)ET(I,L),FOC,BM,COR
      CALL SSWTCH(5,J5)
      IF(J5.EQ.1)GO TO 33
      IF(ABS(COR)-ABS(TOLE*ET(NO,L-1)))202,202,203
  203 ET(NO,L)=ET(NO,L)-COR
      GO TO 36
  202 BM=-BM
      CALL PLOAD(PL(L),BL2,BL,DL,BM,DLC,W)
      CALL SSWTCH(4,J4)
      IF(J4.EQ.1)WRITE(6,105)PL(L)
      DEC(NO)=-(BD+CD+EC-Q(NO)) *D(NO)
      NO1=NO-1
      DO25I=1,NO1
      CALL EBMI(PL(L),S(I),BL,DL,EBM,DLC,W)
      IF(J4.EQ.1)WRITE(6,108)I,EBM
      IF(L.GT.3)GO TO 6
      GO TO 7
    6 ET(I,L)= ET(I,L-3)+3.*(ET(I,L-1)-ET(I,L-2))
```

```
      EB(I,L)= EB(I,L-3)+3.*(EB(I,L-1)-EB(I,L-2))
      GO TO 32
    7 IF(L-2)31,18,31
   18 BOI=EBM/(TI*BE)
      EB(I,2)=EB(I,1)+BOI*(CD+BD-TQ)
      ET(I,2)=ET(I,1)+BOI*(CD-TQ)
      GO TO 32
   31 ET(I,L)=ET(I,L-1)*2.-ET(I,L-2)
      EB(I,L)=EB(I,L-1)*2.-EB(I,L-2)
   32 CALL FMP(NR)
      DEN=DFDET*DMDEB-DMDET*DFDEB
      CEB=(DFDET*BM-DMDET*FOC)/DEN
      CET=(FOC*DMDEB-BM*DFDEB)/DEN
      IF(J4.EQ.1)WRITE(6,105)ET(I,L),EB(I,L),FOC,BM,CEB,CET
      CALL SSWTCH(5,J5)
      IF(J5.EQ.1)GO TO 33
      IF(ABS(CEB)-ABS(TOLE*EB(I,L-1)))16,16,27
   16 IF(ABS(CET)-ABS(TOLE*ET(I,L-1)))25,25,27
   27 EB(I,L)=EB(I,L)-CEB
      ET(I,L)=ET(I,L)-CET
      GO TO 32
   25 DEC(I)=-(BD+CD+EC-Q(I))*D(I)
      CALL INTEG(SI,NO,DEC     ,CEL     )
      FCB=CEL(NO)*2./WL+(P+FD)/(WE*WA)
      STEN=FCB
      CALL PINT(WF,NW,HW,FCB     )
      FCB=FCB*WA
      IF(J4.EQ.1)WRITE(6,105)TF(L),FCB,STEN
      IF(ABS(TF(L)-FCB)-ABS(TOLF*TF(L-1)))71,71,35
   35 IF(KF.EQ.1)GO TO 40
      AS2=TF(L)
      CA2=FCB
      SL=(CA2-CA1)/(AS2-AS1)
      TF(L)=(CA1-SL*AS1)/(1.-SL)
      AS1=AS2
       CA1=CA2
```

```
      GO TO 36
   40 AS1=TF(L)
      CA1=FCB
      TF(L)=.25*(3.*TF(L)+FCB)
      KF=2
      GO TO 36
   71 DCF=TF(L)-P-FD
      GO TO 37
   33 CONTINUE
      END

$IBFTC COMP
C*****COMP -PROGRAM FOR ANALYSIS OF COMPOSITE BEAMS
  102 FORMAT(1X,7E10.2)
  104 FORMAT(1X,7F10.5)
  105 FORMAT(1X,6E15.7)
  106 FORMAT(1X,2I5)
  107 FORMAT(20X,2E15.7)
  108 FORMAT(1X,I7,2E15.8)
  110 FORMAT(72H1RESULTS FROM THE ANALYSIS BY THE RICE UNIVERSITY IBM 70
     140 COMPUTER OF A)
  111 FORMAT(32H SIMPLY-SUPPORTED COMPOSITE BEAM)
  112 FORMAT(17H0 BEAM PROPERTIES/12H01.MATERIALS/15H0   A.STEEL BEAM)
  113 FORMAT(17H    YIELD STRESS=E15.8,18HPSI  YIELD STRAIN=E15.8,6H IN/
     1IN/26H    MODULUS OF ELASTICITY=E15.8,4H PSI)
  137 FORMAT(18H0  B.CONCRETE SLAB)
  114 FORMAT(22H    ULTIMATE STRENGTH=E15.8,4H PSI/32H    STRAIN AT ULTI
     1MATE STRENGTH=E15.8,6H IN/IN)
  138 FORMAT(20H    LIMITING STRAIN=E15.8,6H IN/IN)
  127 FORMAT(20H    TANGENT MODULUS=E15.8)
  117 FORMAT(                                    28H0 2.CROSS SECT
     1ION DIMENSIONS/15H0  A.STEEL BEAM/11H    WEIGHT=E15.8,6H LB/FT)
  118 FORMAT(9H    AREA=E15.8,4H IN2,15X,6HDEPTH=E15.8,3H IN/34H    RECT
     1ANGLES, FROM BOTTOM TO TOP/8H0 NUMBER, 9X,5HDEPTH,10X,5HWIDTH)
  119 FORMAT(                               22H    MOMENT OF INERTIA=E
```

```
   115.8,4H IN4/18H0  B.CONCRETE SLAB)
120 FORMAT(11H    WEIGHT=E15.8,7H LB/FT3,13X,6HDEPTH=E15.8,3H IN/11H
   1  WIDTH =E15.8,3H IN)
122 FORMAT(21H0 3.LINEAR DIMENSIONS/8H    SPAN=E15.8,3H IN13X
   1                   /29H   DISTANCE FROM C/L TO LOAD=E15.8,3H IN)
140 FORMAT(19H0 4. TOTAL WEIGHT =E15.8,3H LB)
123 FORMAT(                                      39H0 5.DEAD LOADS FROM A
   1DJOINING STRUCTURE/17H   ON STEEL BEAM=E15.8,6H LB/FT/21H   ON COM
   2POSITE BEAM=E15.8,6H LB/FT/21H0 6.STRAIN INCREMENT=E15.8,6H IN/IN/
   315H0 8.NODE POINTS)
124 FORMAT(21H    NODE POINT NUMBER,21X,16HX COORDINATE, IN)
125 FORMAT(11X,I5,25X,E15.8)
126 FORMAT(28H0TOLERANCE  USED BY PROGRAM=E15.8)
128 FORMAT(29H0 BEHAVIOR UNDER APPLIED LOAD)
129 FORMAT(8H0  LOAD=E15.8)
130 FORMAT(7H0 NODE ,13HSTRAIN AT TOP,3X,13HSTRAIN AT TOP,3X,9HSTRAIN
   1AT,7X,11HDISTANCE TO)
131 FORMAT(7X,11HOF CONCRETE,5X,14HOF STEEL BEAM,,2X,15HBOTTOM OF STEE
   1L,1X,13HPOINT OF ZERO)
132 FORMAT(7X,11HSLAB, IN/IN,5X,5HIN/IN,11X,11HBEAM, IN/IN,5X,10HSTRAI
   1N, IN)
133 FORMAT(I6,1X,E15.8,1X,E15.8,1X,E15.8,1X,E15.8)
134 FORMAT(7H0 NODE ,9HCHANGE IN,7X,16HCURVATURE, IN-1 ,14HSLOPE, IN/I
   1N  ,2X,13HDEFLECTION,IN)
135 FORMAT(7X,15HCURVATURE, IN-1)
    DIMENSION D0(10),PL(200),S(10),D1(10),ARE(8),DEP(8)
    COMMON BEY,BFY,BE,E0,C1,EE,DH,EC,BA,BD,CD,                   EBM,
   1TOLE,FOC,BM,DFDET,DFDEB,DMDET,DMDEB,     WID(8),DST(8),SE(8),L,I,
   2ET(10,200) ,EB(10,200) ,D2(10),D(10),D2I(10),Q(10),ECT(10),TF(200)
    READ(5,106)NP
    DO33NA=1,NP
    READ(5,104)CD,CB,CW
    READ(5,106)NR
    READ(5,104)(DEP(J),WID(J),J=1,NR)
    DST(1)=0.
    DST(2)=0.
```

```
      BA=0.
      SM=0.
      DO1J=1,NR
      ARE(J)=DEP(J)*WID(J)
      DST(J+1)=DST(J)+DEP(J)
      BA=BA+ARE(J)
    1 SM=SM+ARE(J)*(DST(J)+DEP(J)*.5)
      BW=3.4*BA
      YB =SM/BA
      BI=0.
      DO2J=1,NR
    2 BI=BI+WID(J)*DEP(J)**3/12.+ARE(J)*(YB -(DST(J)+DEP(J)*.5))**2
      BD=DST(NR+1)
      BST=BI/(BD-YB )
      BSB=BI/YB
      READ(5,104)BL,              DL,DPL,TOLE
      READ(5,102)FC,    EU,BFY,BEY
      READ(5,106)NO
      BE=BFY/BEY
      WRITE(6,110)
      WRITE(6,111)
      WRITE(6,112)
      WRITE(6,113)BFY,BEY,BE
      WRITE(6,137)
      F2C=.85*FC
      CT=1.8E6-460.*F2C
      EO=2.*F2C/CT
      WRITE(6,114)FC,EO
      WRITE(6,138)EU
      WRITE(6,127)CT
      WRITE(6,117)    BW
      WRITE(6,118)BA,BD
      WRITE(6,108)(J,DEP(J),WID(J),J=1,NR)
      WRITE(6,119)     BI
      WRITE(6,120)CW,CD,CB
      WRITE(6,122)BL,    DL
```

```
      Z=NO-1
      SI=BL/(2.*Z)
      W=(BW    +CB*CD*CW/144.)/12.
      TW=W    *BL
      READ(5,104)DLS,DLC
      WRITE(6,140)TW
      WRITE(6,123)  DLS,DLC,DPL
      WRITE(6,124)
      DLC=DLC/12.
      W=W+DLS/12.
      DO3I=1,NO
      Z=I-1
      S(I)=Z*SI
      WRITE(6,125)I,S(I)
      EB(I,1)=     W*S(I)*(BL-S(I))*.5/(BSB*BE)
      ET(I,1)=    -W*S(I)*(BL-S(I))*.5/(BST*BE)
      ET(I,1)=    -W*S(I)*(BL-S(I))*BD/(4.*BE*BI)
      D(I)=0.
      ECT(I)=0.
      Q(I)=0.
      D2I(I)=(ET(I,1)-EB(I,1))/BD
    3 D2(I)=D2I(I)
      WRITE(6,126)TOLE
      PL(1)=0.
      EE=EU-EO
      DH=1.+.15*EO/EE
      L=1
      TCA=CD*CB*CT/BE
      TA=TCA+BA
      TQ=(TCA*CD*.5+BA*(CD+BD-YB))/(TA)
      TI=BI+TCA*CD*CD/12.+TCA*(TQ-CD*.5)**2   +BA*(CD+BD-YB-TQ)**2
      EB(NO,2)=DPL+EB(NO,1)
      EBM=(EB(NO,2)-EB(NO,1))*(TI*BE)/(CD+BD-TQ)
      BL2=BL*.5
      ET(NO,2)=ET(NO,1)+EBM*(CD-TQ)/(TI*BE)
      CALL SSWTCH(2,J2)
```

```
      IF(J2.EQ.1)WRITE(6,105)TQ,TI,EB(NO,2),EBM,        ET(NO,2)
      C1=F2C*CB
      WRITE(6,128)
   37 WRITE(6,129)PL(L)
      CALL CSD(SI,NO,D2,D1,D0)
      WRITE(6,130)
      WRITE(6,131)
      WRITE(6,132)
      WRITE(6,133)(J,ECT(J),ET(J,L),EB(J,L), Q(J),J=1,NO)
      WRITE(6,134)
      WRITE(6,135)
      WRITE(6,133)(J, D(J),D2(J),D1(J),D0(J),J=1,NO)
      DO72J=1,NO
      IF(EU-ECT(J))72,72,33
   72 CONTINUE
      L=L+1
      I=NO
      EB(NO,L)=EB(NO,L-1)+DPL
      CALL SSWTCH(3,J3)
      IF(J3.EQ.1)WRITE(6,105)EB(I,L)
      IF(L.GT.3)GO TO 4
      GO TO 5
    4 TF(L)= TF(L-3)+3.*(TF(L-1)-TF(L-2))
      ET(NO,L)= ET(NO,L-3)+3.*(ET(NO,L-1)-ET(NO,L-2))
      GO TO 36
    5 IF(L-2)15,36,15
   15 ET(NO,L)=2.*ET(NO,L-1)-ET(NO,L-2)
   36 EBM=0.
      TF(L)=0.
      CALL FMP(NR)
      COR=FOC/DFDET
      IF(J3.EQ.1)WRITE(6,105)ET(I,L),FOC,BM,COR
      CALL SSWTCH(5,J5)
      IF(J5.EQ.1)GO TO 33
      IF(ABS(COR)-ABS(TOLE*ET(NO,L-1)))202,202,203
  203 ET(NO,L)=ET(NO,L)-COR
```

```
      GO TO 36
  202 BM=-BM
      CALL PLOAD(PL(L),BL2,BL,DL,BM,DLC,W)
      NO1=NO-1
      CALL SSWTCH(4,J4)
      IF(J4.EQ.1)WRITE(6,105)PL(L)
      DO25I=1,NO1
      CALL EBMI(PL(L),S(I),BL,DL,EBM,DLC,W)
      IF(J4.EQ.1)WRITE(6,108)I,EBM
      IF(L.GT.3)GO TO 6
      GO TO 7
    6 ET(I,L)= ET(I,L-3)+3.*(ET(I,L-1)-ET(I,L-2))
      EB(I,L)= EB(I,L-3)+3.*(EB(I,L-1)-EB(I,L-2))
      GO TO 32
    7 IF(L-2)31,18,31
   18 BOI=EBM/(TI*BE)
      EB(I,2)=EB(I,1)+BOI*(CD+BD-TQ)
      ET(I,2)=ET(I,1)+BOI*(CD-TQ)
      GO TO 32
   31 ET(I,L)=ET(I,L-1)*2.-ET(I,L-2)
      EB(I,L)=EB(I,L-1)*2.-EB(I,L-2)
   32 TF(L)=0.
      CALL FMP(NR)
      DEN=DFDET*DMDEB-DMDET*DFDEB
      CEB=(DFDET*BM-DMDET*FOC)/DEN
      CET=(FOC*DMDEB-BM*DFDEB)/DEN
      IF(J4.EQ.1)WRITE(6,105)ET(I,L),EB(I,L),FOC,BM,CEB,CET
      CALL SSWTCH(5,J5)
      IF(J5.EQ.1)GO TO 33
      IF(ABS(CEB)-ABS(TOLE*EB(I,L-1)))16,16,27
   16 IF(ABS(CET)-ABS(TOLE*ET(I,L-1)))25,25,27
   27 EB(I,L)=EB(I,L)-CEB
      ET(I,L)=ET(I,L)-CET
      GO TO 32
   25 CONTINUE
      GO TO 37
```

```
   33 CONTINUE
      END

$IBFTC FMP
C*****FMP-SUBROUTINE FOR FINDING THE INTERNAL FORCE, INTERNAL MOMENT,
C*****AND PARTIAL DERIVATIVES FROM GIVEN STRAIN DISTRIBUTION
      SUBROUTINE FMP(NR)
  105 FORMAT(1X,6E15.8)
  201 FORMAT(6H CASE1)
  202 FORMAT(6H CASE2)
  203 FORMAT(6H CASE3)
  204 FORMAT(6H CASE4)
  205 FORMAT(6H CASE5)
  206 FORMAT(6H CASE6)
  207 FORMAT(6H CASE7)
  208 FORMAT(6H CASE8)
      COMMON BEY,BFY,BE,EO,C1,EE,DH,EC,BA,BD,CD,                   EBM,
     1TOLE,FOC,BM,DFDET,DFDEB,DMDET,DMDEB,     WID(8),DST(8),SE(8),L,I,
     2ET(10,200) ,EB(10,200) ,D2(10),D(10),D2I(10),Q(10),ECT(10),TF(200)
      D2(I)=(ET(I,L)-EB(I,L))/BD
      IF(ABS(ET(I,L)-ET(I,1))-ABS(TOLE*ET(I,1)))11,11,12
   11 FOC=0.
      BM=0.
      DFDET=0.
      DFDEB=0.
      DMDET=0.
      DMDEB=0.
      GO TO 13
   12 D(I)=D2(I)-D2I(I)
      Q(I)=(ET(I,L)-ET(I,1))/D(I)+CD
      ECT(I)=Q(I)*D(I)
      IF(ECT(I))14,11,11
   14 YO=EO/D(I)
      BT=Q(I)-CD
      C2=D(I)/EO
```

```
      DET=ET(I,L)-ET(I,1)
      DQDB= DET/(BD*D(I)*D(I))
      DQDT=-DQDB+1./D(I)
      D1Q=C2*Q(I)*(2.-C2*Q(I))
      D3Q=D1Q*Q(I)
      D2Q=DH-.15*D(I)*Q(I)/EE
      D4Q=D2Q*Q(I)
      D1B=C2*BT*(2.-C2*BT)
      D3B=BT*D1B
      D2B=DH-.15*D(I)*BT/EE
      D4B=D2B*BT
      IF(BT      )94,94,96
   94 Y1=0.
      IF(EO-ECT(I))95,95,4
   95 Y2=Q(I)
      Y3=0.
      Y4=0.
      DFDET=D1Q*DQDT
      DFDEB=D1Q*DQDB
      DMDET=D3Q*DQDT
      DMDEB=D3Q*DQDB
      GO TO 5
    4 Y2=YO
      Y3=YO
      Y4=Q(I)
      DFDET=D2Q*DQDT
      DFDEB=D2Q*DQDB
      DMDET=D4Q*DQDT
      DMDEB=D4Q*DQDB
      GO TO 5
   96 ECB=BT*D(I)
      IF(EO-ECB)6,7,7
    6 Y1=BT
      IF(EO-ECT(I))8,8,9
    8 Y2=Q(I)
      Y3=0.
```

```
      Y4=0.
      DFDET=(D1Q-D1B)*DQDT
      DFDEB=(D1Q-D1B)*DQDB
      DMDET=(D3Q-D3B)*DQDT
      DMDEB=(D3Q-D3B)*DQDB
      GO TO 5
    9 Y2=YO
      Y3=YO
      Y4=Q(I)
      DFDET=          DQDT*(D2Q-D1B)
      DFDEB=          DQDB*(D2Q-D1B)
      DMDET=          DQDT*(D4Q-D3B)
      DMDEB=          DQDB*(D4Q-D3B)
      GO TO 5
    7 Y1=0.
      Y2=0.
      Y3=BT
      Y4=Q(I)
      DFDET=DQDT*(D2Q-D2B)
      DFDEB=DQDB*(D2Q-D2B)
      DMDET=DQDT*(D4Q-D4B)
      DMDEB=DQDB*(D4Q-D4B)
    5 DQ=EC+BD+CD-Q(I)
      Y21=Y2-Y1
      Y22=Y2*Y2-Y1*Y1
      Y23=Y2*Y2*Y2-Y1*Y1*Y1
      Y24=Y2*Y2*Y2*Y2-Y1*Y1*Y1*Y1
      Y41=Y4-Y3
      Y42=Y4*Y4-Y3*Y3
      Y43=Y4*Y4*Y4-Y3*Y3*Y3
      FOC=C1*(C2*(Y22-C2*Y23/3.)+DH*Y41- .075*Y42*D(I)/EE)
      POF=((Y22-2.*C2*Y23/3.)/EO-.075*Y42/EE)/BD
      DFDET=C1*(DFLET+POF)
      DFDEB=C1*(DFDEB-POF)
      BM=C1*(C2*(2.*Y23/3.-C2*Y24/4.)+DH*Y42*.5-.05*D(I)*Y43/EE)+FOC*DQ
      POM=((2.*Y23/3.-.5*C2*Y24)/EO-.05*Y43/EE)/BD
```

```
      DMDET=C1*(DMDET+POM)+DFDET*DQ-FOC*DQDT
      DMDEB=C1*(DMDEB-POM)+DFDEB*DQ-FOC*DQDB
      CALL SSWTCH(6,J6)
      IF(J6.EQ.1)WRITE(6,105)FOC,BM,DFDET,DFDEB,DMDET,DMDEB
   13 SE(1)=EB(I,L)
      SE(NR+1)=ET(I,L)
      DO39J=2,NR
   39 SE(J)=SE(1)+DST(J)*D2(I)
      IF(J6.EQ.1)WRITE(6,105)(SE(J),J=1,NR)
      DO60K=1,NR
      IF((SE(K).LT. BEY).AND.(SE(K+1).GT.-BEY).AND.
     1(SE(K).GT.-BEY).AND.(SF(K+1).LT. BEY)) GO TO 21
      IF((SE(K).GT. BEY).AND.(SE(K+1).GT. BEY).OR.
     1(SE(K).LT.-BEY).AND.(SE(K+1).LT.-BEY)) GO TO 22
      YC=-(BEY+EB(I,L))/D2(I)
      YT= (BEY-EB(I,L))/D2(I)
      IF((SE(K).GT. BEY).AND.(SE(K+1).GT.-BEY).AND.
     1                          (SE(K+1).LT. BEY)) GO TO 23
      IF((SE(K).LT. BEY).AND.(SE(K+1).LT.-BEY).AND.
     1(SE(K).GT.-BEY))GO TO 24
      IF((SE(K).GT. BEY).AND.(SE(K+1).LT.-BEY))GO TO 25
      IF((SE(K).LT.-BEY).AND.(SE(K+1).GT.-BEY).AND.
     1(SE(K+1).LT.BEY))GO TO 26
      IF((SE(K).GT.-BEY).AND.(SE(K+1).GT. BEY).AND.
     1(SE(K).LT. BEY))GO TO 27
      CALL STP(WID(K),YT,DST(K+1),SE(K+1))
      CALL STE(WID(K),YC,YT)
      CALL STP(WID(K),DST(K),YC,SE(K))
      IF(J6.EQ.1)GO TO 218
      GO TO 60
  218 WRITE(6,208)
      WRITE(6,105)FOC,BM,DFDET,DFDEB,DMDET,DMDEB
      GO TO 60
   21 CALL STE(WID(K),DST(K),DST(K+1))
      IF(J6.EQ.1)GO TO 211
      GO TO 60
```

```
  211 WRITE(6,201)
      WRITE(6,105)FOC,BM,DFDET,DFDEB,DMDET,DMDEB
      GO TO 60
   22 CALL STP(WID(K),DST(K),DST(K+1),SE(K))
      IF(J6.EQ.1)GO TO 212
      GO TO 60
  212 WRITE(6,202)
      WRITE(6,105)FOC,BM,DFDET,DFDEB,DMDET,DMDEB
      GO TO 60
   23 CALL STE(WID(K),YT,DST(K+1))
      CALL STP(WID(K),DST(K),YT,SE(K))
      IF(J6.EQ.1)GO TO 213
      GO TO 60
  213 WRITE(6,203)
      WRITE(6,105)FOC,BM,DFDET,DFDEB,DMDET,DMDEB
      GO TO 60
   24 CALL STE(WID(K),DST(K),YC)
      CALL STP(WID(K),YC,DST(K+1),SE(K+1))
      IF(J6.EQ.1)GO TO 214
      GO TO 60
  214 WRITE(6,204)
      WRITE(6,105)FOC,BM,DFDET,DFDEB,DMDET,DMDEB
      GO TO 60
   25 CALL STP(WID(K),YC,DST(K+1),SE(K+1))
      CALL STE(WID(K),YT,YC)
      CALL STP(WID(K),DST(K),YT,SE(K))
      IF(J6.EQ.1)GO TO 215
      GO TO 60
  215 WRITE(6,205)
      WRITE(6,105)FOC,BM,DFDET,DFDEB,DMDET,DMDEB
      GO TO 60
   26 CALL STE(WID(K),YC,DST(K+1))
      CALL STP(WID(K),DST(K),YC,SE(K))
      IF(J6.EQ.1)GO TO 216
      GO TO 60
  216 WRITE(6,206)
```

```
      WRITE(6,105)FOC,BM,DFDET,DFDEB,DMDET,DMDEB
      GO TO 60
   27 CALL STP(WID(K),YT,DST(K+1),SE(K+1))
      CALL STE(WID(K),DST(K),YT)
      IF(J6.EQ.1)GO TO 217
      GO TO 60
  217 WRITE(6,207)
      WRITE(6,105)FOC,BM,DFDET,DFDEB,DMDET,DMDEB
   60 CONTINUE
      FOC=FOC+TF(L)
      BM=BM+EBM
      RETURN
      END

$IBFTC PLOAD
C*****PLOAD-SUBROUTINE WHICH CALCULATES EXTERNAL LOAD FROM EXTERNAL MOMENT
C*****FOR H20-S16-44 LANE LOADING
      SUBROUTINE PLOAD(PLO,DN,BL,DL,EBM,DLC,W)
      Q=W+DLC
      PLO=(EBM-Q  *DN*.5*(BL-DN))/(DN*(.5+.04  *(BL-DN)/27.))
      RETURN
      END

$IBFTC EBMI
C*****EBMI-SUBROUTINE WHICH CALCULATES  EXTERNAL MOMENT FROM EXTERNAL LOAD
C*****FOR H20-S16-44 LANE LOADING
      SUBROUTINE  EBMI(PLO,DN,BL,DL,EBM,DLC,W)
      Q=W+DLC
      EBM=PLO*DN*(.5+ .04 *(BL-DN)/27.)+Q  *DN*.5*(BL-DN)
      RETURN
      END
```

```
$IBFTC PLOAD
C*****PLOAD-SUBROUTINE WHICH CALCULATES EXTERNAL LOAD FROM EXTERNAL MOMENT
C*****FOR A UNIFORMLY DISTRIBUTED LOAD
      SUBROUTINE PLOAD(PLO,DN,BL,DL,EBM,DLC,W)
      Q=DLC+W
      PLO=EBM/(DN*.5*(BL-DN))-Q
      RETURN
      END

$IBFTC EBMI
C*****EBMI-SUBROUTINE WHICH CALCULATES  EXTERNAL MOMENT FROM EXTERNAL LOAD
C*****FOR A UNIFORMLY DISTRIBUTED LOAD
      SUBROUTINE  EBMI(PLO,DN,BL,DL,EBM,DLC,W)
      Q=DLC+W
      EBM=(PLO+Q  )*DN*.5*(BL-DN)
      RETURN
      END

$IBFTC PLOAD
C*****PLOAD-SUBROUTINE WHICH CALCULATES EXTERNAL LOAD FROM EXTERNAL MOMENT
C*****FOR TWO EQUALLY SPACED SYMMETRICAL  CONCENTRATED LOADS
      SUBROUTINE PLOAD(PLO,DN,BL,DL,EBM,DLC,W)
      EBM=EBM-(W+DLC)*DN*.5*(BL-DN)
      IF(DN-BL*.5+DL)91,92,92
   92 PLO= EBM/(.5*BL-DL)
      GO TO 93
   91 PLO= EBM/DN
   93 CONTINUE
      RETURN
      END

$IBFTC EBMI
C*****EBMI-SUBROUTINE WHICH CALCULATES  EXTERNAL MOMENT FROM EXTERNAL LOAD
```

```
C*****FOR TWO EQUALLY SPACED SYMMETRICAL  CONCENTRATED LOADS
      SUBROUTINE EBMI(PLO,DN,BL,DL,EBM,DLC,W)
      Q=(W+DLC)*DN*.5*(BL-DN)
      IF(DN-BL/2.+DL)91,92,92
   92 EBM=PLO*(.5*BL-DL)+Q
      GO TO 93
   91 EBM=PLO*DN+Q
   93 CONTINUE
      RETURN
      END

$IBFTC PLOAD
C*****PLOAD-SUBROUTINE WHICH CALCULATES EXTERNAL LOAD FROM EXTERNAL MOMENT
C*****FOR A SINGLE CONCENTRATED LOAD AT MIDSPAN
      SUBROUTINE PLOAD(PLO,DN,BL,DL,EBM,DLC,W)
      Q=W+DLC
      PLO=(EBM-Q*DN*.5(BL-DN))*2./DN
      RETURN
      END

$IBFTC EBMI
C*****EBMI-SUBROUTINE WHICH CALCULATES  EXTERNAL MOMENT FROM EXTERNAL LOAD
C*****FOR A SINGLE CONCENTRATED LOAD AT MIDSPAN
      SUBROUTINE  EBMI(PLO,DN,BL,DL,EBM,DLC,W)
      Q=W+DLC
      EBM=PLO*DN*.5+Q*DN*.5*(BL-DN)
      RETURN
      END

$IBFTC CSD
C*****CSD-SUBROUTINE WHICH CALCULATES THE SLOPES AND DEFLECTIONS AT EACH
C*****NODE POINT FROM THE CURVATURES
      SUBROUTINE CSD(SI,NO,D2,D1,D0)
```

```
      DIMENSION D2(10),D1(10),D0(10)
      CALL INTEG(SI,NO,D2,D1)
      CALL SLOPE(SI,NO,D1)
      CALL INTEG(SI,NO,D1,D0)
      RETURN
      END

$IBFTC INTEG
C*****INTEG-NUMERICAL INTEGRATION SUBROUTINE
      SUBROUTINE INTEG(H,N,F,G)
      DIMENSION F(10),G(10)
      Z1=F(N-1)
      Z2=F(N-2)
      G(1)=0.
      KJ=N-1
      DO3J=2,KJ
    3 G(J)=G(J-1)+H*(5.*F(J-1)+8.*F(J)-F(J+1))/12.
      G(N)=G(N-1)+H*(5.*F(N)+8.*Z1-Z2)/12.
      RETURN
      END

$IBFTC PINT
C*****PINT-PARABOLIC INTERPOLATION SUBROUTINE
      SUBROUTINE PINT(F,N,HF,G)
      DIMENSION F(10)
      L=G/HF+1.
      TL=L-1
      G=G-TL*HF
      IF(L-N+1)80,81,80
   81 T=F(N-1)
      F(N+1)=F(N-1)
      F(N+2)=F(N-2)
      L=N
      G=HF-G
```

```
      GO TO 80
   80 G=G*G*(F(L)-2.*F(L+1)+F(L+2))/(2.*HF*HF)+G*(-3.*F(L)+4.*F(L+1)-
     1F(L+2))/(2.*HF)+F(L)
      RETURN
      END

$IBFTC SLOPE
C*****SLOPE-SUBROUTINE WHICH CALCULATES SLOPES AT EACH NODE POINT FROM
C*****THE CURVATURES
      SUBROUTINE SLOPE(H,N,F)
      DIMENSION F(10)
      C=-F(N)
      DO11 J=1,N
   11 F(J)=F(J)+C
      RETURN
      END

$IBFTC STE
C*****STE-SUBROUTINE WHICH FINDS THE INTERNAL FORCE,INTERNAL MOMENT, AND
C*****PARTIAL DERIVATIVES OVER AN ELASTIC ELEMENT OF THE STEEL BEAM
      SUBROUTINE STE(B,Y1,Y2)
      COMMON BEY,BFY,BE,EO,C1,EE,DH,EC,BA,BD,CD,                      EBM,
     1TOLE,FOC,BM,DFDET,DFDEB,DMDET,DMDEB,      WID(8),DST(8),SE(8),L,I,
     2ET(10,200) ,EB(10,200),PHI(10),D(10),D2I(10),Q(10),ECT(10),TF(200)
      BBE=B*BE
      Y21=Y2-Y1
      Y22=(Y2*Y2-Y1*Y1)*.5
      Y23=(Y2*Y2*Y2-Y1*Y1*Y1)/3.
      FB=BBE*(EB(I,L)*Y21+PHI(I)*Y22)
      BM=BM+FB*EC+BBE*(EB(I,L)*Y22   +PHI(I)*Y23)
      FOC=FOC+FB
      PFT=BBE*Y22/BD
      PFB=BBE*Y21-PFT
      PMT=BBE*Y23/BD+EC*PFT
```

```
      PMB=BBE*Y22-PMT+EC*PFB
      DFDET=DFDET+PFT
      DFDEB=DFDEB+PFB
      DMDET=DMDET+PMT
      DMDEB=DMDEB+PMB
      RETURN
      END

$IBFTC STP
C*****STP-SUBROUTINE WHICH FINDS THE INTERNAL FORCE AND INTERNAL MOMENT
C*****OVER A PLASTIC ELEMENT OF THE STEEL BEAM
      SUBROUTINE STP(B,Y3,Y4,S)
      COMMON BEY,BFY,BE,EO,C1,EE,DH,EC,BA,BD,CD,                   EBM,
     1TOLE,FOC,BM,DFDET,DFDEB,DMDET,DMDEB,     WID(8),DST(8),SE(8),L,I,
     2ET(10,200) ,EB(10,200) ,D2(10),D(10),D2I(10),Q(10),ECT(10),TF(200)
      DD=Y4-Y3
      FB=BFY*DD*B
      IF(S.LT.0.)FB=-FB
      BM=BM+FB*(EC+Y3+DD*.5)
      FOC=FOC+FB
      RETURN
      END
```